Research on Priority Areas and Grant-in-Aid for Scientific Research (B), Grand-in-Aid for Exploratory Research, Specially Designated Research Promotion, Takeda Science Foundation, Senri Life Science Foundation, The Uehara Memorial Foundation and Mochida Memorial Foundation for Medical and Pharmaceutical Research. A part of this work was supported by the Nanotechnology Network Project of the Ministry of Education, Culture, Sports, Science and Technology Japan at the Research Center for Ultrahigh-Voltage Electron Microscopy, Osaka University (Handai Multi-functional Nano-Foundry).

## AUTHOR CONTRIBUTIONS

S.S. and T. Furukawa designed the project. S.S., Y.O. and K. Katoh carried out the molecular, immunocytochemistry and electron microscopy experiments. S.S., M.K., K.M. and T.K. carried out the ERG experiments. S.S., A.T. and T. Furukawa produced the knockout mice. S.S. and N.K. performed the electron tomography analysis. J.U. carried out the immuno–electron microscopy experiments. S.S. and K.F. performed the OKR experiments. T.M. and H.S. carried out the VEP experiments. S.S., Y.O., M.K., K. Kobayashi and T.T. conducted the pull-down experiments. S.S., Y.O. and T. Furukawa wrote the manuscript. Y.T., T. Fujikado. and T. Furukawa supervised the project.

Published online at http://www.nature.com/natureneuroscience/
Reprints and permissions information is available online at http://npg.nature.com/reprintsandpermissions/

1. Waites, C.L., Craig, A.M. & Garner, C.C. Mechanisms of vertebrate synaptogenesis. *Annu. Rev. Neurosci.* **28**, 251–274 (2005).
2. Sudhof, T.C. The synaptic vesicle cycle. *Annu. Rev. Neurosci.* **27**, 509–547 (2004).
3. tom Dieck, S. & Brandstatter, J.H. Ribbon synapses of the retina. *Cell Tissue Res.* **326**, 339–346 (2006).
4. Sterling, P. & Matthews, G. Structure and function of ribbon synapses. *Trends Neurosci.* **28**, 20–29 (2005).
5. Straub, V. & Campbell, K.P. Muscular dystrophies and the dystrophin-glycoprotein complex. *Curr. Opin. Neurol.* **10**, 168–175 (1997).
6. Henry, M.D. & Campbell, K.P. Dystroglycan inside and out. *Curr. Opin. Cell Biol.* **11**, 602–607 (1999).
7. Ibraghimov-Beskrovnaya, O. *et al.* Primary structure of dystrophin-associated glycoproteins linking dystrophin to the extracellular matrix. *Nature* **355**, 696–702 (1992).
8. Sugiyama, J., Bowen, D.C. & Hall, Z.W. Dystroglycan binds nerve and muscle agrin. *Neuron* **13**, 103–115 (1994).
9. Winder, S.J. The complexities of dystroglycan. *Trends Biochem. Sci.* **26**, 118–124 (2001).
10. Talts, J.F., Andac, Z., Gohring, W., Brancaccio, A. & Timpl, R. Binding of the G domains of laminin α1 and α2 chains and perlecan to heparin, sulfatides, α-dystroglycan and several extracellular matrix proteins. *EMBO J.* **18**, 863–870 (1999).
11. Sugita, S. *et al.* A stoichiometric complex of neurexins and dystroglycan in brain. *J. Cell Biol.* **154**, 435–445 (2001).
12. Ueda, H., Gohdo, T. & Ohno, S. β-dystroglycan localization in the photoreceptor and Muller cells in the rat retina revealed by immunoelectron microscopy. *J. Histochem. Cytochem.* **46**, 185–191 (1998).
13. Jastrow, H., Koulen, P., Altrock, W.D. & Kroger, S. Identification of a β-dystroglycan–immunoreactive subcompartment in photoreceptor terminals. *Invest. Ophthalmol. Vis. Sci.* **47**, 17–24 (2006).
14. Schmitz, F. & Drenckhahn, D. Localization of dystrophin and β-dystroglycan in bovine retinal photoreceptor processes extending into the postsynaptic dendritic complex. *Histochem. Cell Biol.* **108**, 249–255 (1997).
15. Dalloz, C. *et al.* Differential distribution of the members of the dystrophin glycoprotein complex in mouse retina: effect of the *mdx(3Cv)* mutation. *Mol. Cell. Neurosci.* **17**, 908–920 (2001).
16. Cibis, G.W., Fitzgerald, K.M., Harris, D.J., Rothberg, P.G. & Rupani, M. The effects of dystrophin gene mutations on the ERG in mice and humans. *Invest. Ophthalmol. Vis. Sci.* **34**, 3646–3652 (1993).
17. Fitzgerald, K.M., Cibis, G.W., Giambrone, S.A. & Harris, D.J. Retinal signal transmission in Duchenne muscular dystrophy: evidence for dysfunction in the photoreceptor/depolarizing bipolar cell pathway. *J. Clin. Invest.* **93**, 2425–2430 (1994).
18. Pillers, D.A. Dystrophin and the retina. *Mol. Genet. Metab.* **68**, 304–309 (1999).
19. Nishida, A. *et al. Otx2* homeobox gene controls retinal photoreceptor cell fate and pineal gland development. *Nat. Neurosci.* **6**, 1255–1263 (2003).
20. Koike, C. *et al.* Functional roles of Otx2 transcription factor in postnatal mouse retinal development. *Mol. Cell Biol.* **27**, 8318–8329 (2007).
21. Carter-Dawson, L.D. & LaVail, M.M. Rods and cones in the mouse retina. I. Structural analysis using light and electron microscopy. *J. Comp. Neurol.* **188**, 245–262 (1979).
22. Iwasaki, M., Myers, K.M., Rayborn, M.E. & Hollyfield, J.G. Interphotoreceptor matrix in the human retina: cone-like domains surround a small population of rod photoreceptors. *J. Comp. Neurol.* **319**, 277–284 (1992).
23. Dick, O. *et al.* The presynaptic active zone protein bassoon is essential for photoreceptor ribbon synapse formation in the retina. *Neuron* **37**, 775–786 (2003).
24. Schmitz, F., Konigstorfer, A. & Sudhof, T.C. RIBEYE, a component of synaptic ribbons: a protein's journey through evolution provides insight into synaptic ribbon function. *Neuron* **28**, 857–872 (2000).
25. Nomura, A. *et al.* Developmentally regulated postsynaptic localization of a metabotropic glutamate receptor in rat rod bipolar cells. *Cell* **77**, 361–369 (1994).
26. Rao-Mirotznik, R., Harkins, A.B., Buchsbaum, G. & Sterling, P. Mammalian rod terminal: architecture of a binary synapse. *Neuron* **14**, 561–569 (1995).
27. Robson, J.G. & Frishman, L.J. Response linearity and kinetics of the cat retina: the bipolar cell component of the dark-adapted electroretinogram. *Vis. Neurosci.* **12**, 837–850 (1995).
28. Pillers, D.A. *et al.* Dystrophin expression in the human retina is required for normal function as defined by electroretinography. *Nat. Genet.* **4**, 82–86 (1993).
29. Sigesmund, D.A. *et al.* Characterization of the ocular phenotype of Duchenne and Becker muscular dystrophy. *Ophthalmology* **101**, 856–865 (1994).
30. Holzfeind, P.J. *et al.* Skeletal, cardiac and tongue muscle pathology, defective retinal transmission, and neuronal migration defects in the *Large* (*myd*) mouse defines a natural model for glycosylation-deficient muscle-eye-brain disorders. *Hum. Mol. Genet.* **11**, 2673–2687 (2002).
31. Hohenester, E., Tisi, D., Talts, J.F. & Timpl, R. The crystal structure of a laminin G-like module reveals the molecular basis of α-dystroglycan binding to laminins, perlecan and agrin. *Mol. Cell* **4**, 783–792 (1999).
32. Bowe, M.A., Deyst, K.A., Leszyk, J.D. & Fallon, J.R. Identification and purification of an agrin receptor from Torpedo postsynaptic membranes: a heteromeric complex related to the dystroglycans. *Neuron* **12**, 1173–1180 (1994).
33. Ervasti, J.M. & Campbell, K.P. A role for the dystrophin-glycoprotein complex as a transmembrane linker between laminin and actin. *J. Cell Biol.* **122**, 809–823 (1993).
34. Kanagawa, M. *et al.* Disruption of perlecan binding and matrix assembly by post-translational or genetic disruption of dystroglycan function. *FEBS Lett.* **579**, 4792–4796 (2005).
35. Michele, D.E. *et al.* Post-translational disruption of dystroglycan-ligand interactions in congenital muscular dystrophies. *Nature* **418**, 417–422 (2002).
36. Prakash, S., Caldwell, J.C., Eberl, D.F. & Clandinin, T.R. *Drosophila* N-cadherin mediates an attractive interaction between photoreceptor axons and their targets. *Nat. Neurosci.* **8**, 443–450 (2005).
37. Bozdagi, O., Valcin, M., Poskanzer, K., Tanaka, H. & Benson, D.L. Temporally distinct demands for classic cadherins in synapse formation and maturation. *Mol. Cell. Neurosci.* **27**, 509–521 (2004).
38. Sanes, J.R. & Lichtman, J.W. Induction, assembly, maturation and maintenance of a postsynaptic apparatus. *Nat. Rev. Neurosci.* **2**, 791–805 (2001).
39. Gee, S.H., Montanaro, F., Lindenbaum, M.H. & Carbonetto, S. Dystroglycan-α, a dystrophin-associated glycoprotein, is a functional agrin receptor. *Cell* **77**, 675–686 (1994).
40. Ervasti, J.M. & Campbell, K.P. Membrane organization of the dystrophin-glycoprotein complex. *Cell* **66**, 1121–1131 (1991).
41. Zaccaria, M.L., Di Tommaso, F., Brancaccio, A., Paggi, P. & Petrucci, T.C. Dystroglycan distribution in adult mouse brain: a light and electron microscopy study. *Neuroscience* **104**, 311–324 (2001).
42. Deng, C., Wynshaw-Boris, A., Zhou, F., Kuo, A. & Leder, P. Fibroblast growth factor receptor 3 is a negative regulator of bone growth. *Cell* **84**, 911–921 (1996).

THE JOURNAL OF BIOLOGICAL CHEMISTRY VOL. 283, NO. 38, pp. 26188–26197, September 19, 2008


# Heat Shock Transcription Factor 1-activating Compounds Suppress Polyglutamine-induced Neurodegeneration through Induction of Multiple Molecular Chaperones*

Received for publication, December 26, 2007, and in revised form, July 14, 2008 Published, JBC Papers in Press, July 16, 2008, DOI 10.1074/jbc.M710521200

**Nobuhiro Fujikake**[‡1,2], **Yoshitaka Nagai**[‡1,2,3], **H. Akiko Popiel**[‡2], **Yuma Okamoto**[‡2], **Masamitsu Yamaguchi**[§], **and Tatsushi Toda**[‡]

*From the* [‡]*Division of Clinical Genetics, Department of Medical Genetics, Osaka University Graduate School of Medicine, Suita, Osaka 565-0871, Japan and the* [§]*Department of Applied Biology, Kyoto Institute of Technology, Sakyo-ku, Kyoto 606-8585, Japan*

Many neurodegenerative diseases including Alzheimer, Parkinson, and polyglutamine (polyQ) diseases are thought to be caused by protein misfolding. The polyQ diseases, including Huntington disease and spinocerebellar ataxias (SCAs), are caused by abnormal expansions of the polyQ stretch in disease-causing proteins, which trigger misfolding of these proteins, resulting in their deposition as inclusion bodies in affected neurons. Although genetic expression of molecular chaperones has been shown to suppress polyQ protein misfolding and neurodegeneration, toward developing a therapy, it is ideal to induce endogenous molecular chaperones by chemical administration. In this study, we assessed the therapeutic effects of heat shock transcription factor 1 (HSF1)-activating compounds, which induce multiple molecular chaperones, on polyQ-induced neurodegeneration *in vivo*. We found that oral administration of 17-(allylamino)-17-demethoxygeldanamycin (17-AAG) markedly suppresses compound eye degeneration and inclusion body formation in a *Drosophila* model of SCA. 17-AAG also dramatically rescued the lethality of the SCA model (74.1% rescue) and suppressed neurodegeneration in a Huntington disease model (46.3% rescue), indicating that 17-AAG is widely effective against various polyQ diseases. 17-AAG induced Hsp70, Hsp40, and Hsp90 expression in a dose-dependent manner, and the expression levels correlated with its therapeutic effects. Furthermore, knockdown of HSF1 abolished the induction of molecular chaperones and the therapeutic effect of 17-AAG, indicating that its therapeutic effects depend on HSF1 activation. Our study indicates that induction of multiple molecular chaperones by 17-AAG treatment is a promising therapeutic approach for a wide range of polyQ diseases and possibly other neurodegenerative diseases.

The accumulation and deposition of misfolded proteins in the brain has been recognized as a common molecular pathogenesis of various neurodegenerative diseases including Alzheimer disease, Parkinson disease, amyotrophic lateral sclerosis, and the polyglutamine (polyQ)[4] diseases, and hence these diseases are called protein misfolding diseases (1). Indeed, most genetic mutations responsible for these diseases produce mutant proteins that are prone to be misfolded. These facts strongly indicate that protein misfolding commonly occurs as the initial step in the pathogenic cascade of neurodegenerative diseases, and hence protein misfolding is considered to be a common therapeutic target for these neurodegenerative diseases.

The polyQ diseases are a group of inherited neurodegenerative diseases including Huntington disease, various types of spinocerebellar ataxia (SCA1, 2, 6, 7, and 17 and SCA3/MJD), dentatorubral-pallidoluysian atrophy, and spinobulbar muscular atrophy, all of which are caused by expansions of the polyQ stretch to greater than 35–40 repeats in each disease-causing protein (2, 3). These expanded polyQ stretches cause misfolding of the disease-causing proteins, leading to their pathogenic interactions with themselves (aggregation) or other cellular proteins, resulting in their deposition and recruitment as inclusion bodies in affected neurons (1). The pathogenic interactions of misfolded polyQ proteins with other cellular proteins such as transcription factors, proteasome subunits, and cytoskeletal proteins have been reported to cause dysfunction of these proteins, eventually leading to neuronal dysfunction (4–6). Although therapeutic approaches against the dysfunction of each of these cellular proteins have been proposed to date, such as histone deacetylase inhibitors to improve transcriptional dysregulation (7), their therapeutic effects were limited because polyQ-induced neuronal dysfunction results from the dysfunction of multiple cellular proteins (2). In contrast, misfolding of the polyQ protein is likely the initial event in the pathogenic cascade, and hence suppression of protein misfolding is expected to inhibit a wide range of multiple downstream

* This work was supported in part by Grants-in-Aid for Scientific Research on Priority Areas (to Y. N.; Advanced Brain Science Project, Research on Pathomechanisms of Brain Disorders, Life of Proteins, and Protein Community) from the Ministry of Education, Culture, Sports, Science, and Technology, Japan; by a Grant-in-Aid for the Research Committee for Ataxic Diseases (to Y. N.) from the Ministry of Health, Labor and Welfare, Japan; and by Grants-in-Aid for Scientific Research (B) (to Y. N.) and for Young Scientists (B) (to N. F.) from the Japan Society for the Promotion of Science. The costs of publication of this article were defrayed in part by the payment of page charges. This article must therefore be hereby marked "*advertisement*" in accordance with 18 U.S.C. Section 1734 solely to indicate this fact.

[1] These authors contributed equally to this work.
[2] Present address: Dept. of Degenerative Neurological Diseases, National Center of Neurology and Psychiatry, Kodaira, Tokyo 187-8502, Japan.
[3] To whom correspondence should be addressed. Tel.: 81-6-6879-3381; Fax: 81-6-6879-3389; E-mail: nagai@clgene.med.osaka-u.ac.jp.

[4] The abbreviations used are: polyQ, polyglutamine; SCA, spinocerebellar ataxia; HSF1, heat shock transcription factor 1; 17-AAG, 17-(allylamino)-17-demethoxygeldanamycin; GA, geldanamycin; RA, radicicol; CL, celastrol; SB, sodium butyrate; GGA, geranylgeranylacetone; HA, hemagglutinin; SL2, Schneider line 2; HRP, horseradish peroxidase; RT, reverse transcription; RNAi, RNA interference.

events, resulting in the most effective suppression of neuronal dysfunction.

Molecular chaperones are known to suppress protein misfolding by synergistically assisting misfolded proteins in the refolding process, as well as newly synthesized proteins in the folding process. For example, Hsp70 has been reported to act in concert with Hsp40 to suppress misfolding of various polyQ proteins *in vitro*, resulting in suppression of their aggregation (8, 9). In a *Drosophila* model of the polyQ diseases, co-expression of Hsp70 and Hsp40 has been reported to synergistically suppress misfolding of the polyQ protein, resulting in remarkable suppression of polyQ-induced neurodegeneration, although expression of Hsp70 or Hsp40 alone exhibits weaker suppression (10–12). Furthermore, genetic expression of Hsp70 or Hsp40 alone is known to cause cytotoxicity to unstressed cells, which is not observed when both chaperones are co-expressed (10, 13), suggesting that the balance of the amounts of molecular chaperones is important for their proper function (14). In addition, expression of other molecular chaperones such as Hsp90, Hsp105, and Hsp27 is also reported to suppress polyQ-induced cytotoxicity in cell culture models (15–17). Based on these results, expression of multiple molecular chaperones is expected to synergistically suppress polyQ-induced neurodegeneration and to have low cytotoxicity to unstressed cells.

Expression of molecular chaperones upon exposure to various types of cellular stress is known to be regulated by heat shock transcription factor 1 (HSF1). Under unstressed conditions, HSF1 is localized in the cytosol and is inactivated in a protein complex including Hsp90 (18). Upon exposure to stress, HSF1 dissociates from the Hsp90 protein complex, translocates into the nucleus, and binds to the heat shock element in the promoter region of various molecular chaperone genes to simultaneously induce their expression (19). Activation of HSF1 is regulated through various post-translational modifications such as phosphorylation, as well as alternative splicing (20, 21). In fact, HSF1 is phosphorylated in response to heat shock stress in HeLa cells and induces multiple molecular chaperones such as Hsp70 and Hsp40, which confer tolerance against heat shock stress on the cells (22, 23). Furthermore, expression of a constitutively active mutant of HSF1, which lacks the regulatory domain that binds to the Hsp90 protein complex, has been reported to suppress polyQ protein misfolding through induction of molecular chaperones (24). Therefore, HSF1 has been considered to be an attractive therapeutic target for the polyQ diseases.

Although genetic expression of molecular chaperones and a constitutively active mutant of HSF1 ameliorates polyQ-induced phenotypes *in vivo* (11, 12, 24), delivery of exogenous genes into the human brain is extremely limited. As a next step toward developing a therapy, it is ideal to pharmacologically induce endogenous molecular chaperones by administration of small chemical compounds, instead of to express exogenous genes. Interestingly, some compounds are known to activate HSF1 and to induce multiple endogenous molecular chaperones even under unstressed conditions (25). These include Hsp90 inhibitors, which dissociate HSF1 from the Hsp90 protein complex, and protein kinase C activators, which promote the phosphorylation of HSF1, both leading to activation of HSF1 (18, 26).

In this study, we investigated the therapeutic effects of administration of various HSF1-activating compounds on polyQ-induced neurodegeneration *in vivo*. We here show that oral administration of 17-(allylamino)-17-demethoxygeldanamycin (17-AAG), a derivative of geldanamycin, markedly suppresses polyQ-induced neurodegeneration in *Drosophila* models of two polyQ diseases through induction of multiple molecular chaperones. Our study indicates the potential of HSF1-activating compounds as therapeutic candidates for a wide range of polyQ diseases as well as other neurodegenerative diseases.

## EXPERIMENTAL PROCEDURES

*Fly Stocks and Treatment*—Flies were cultured and crossed under standard conditions at 25 °C. Transgenic fly lines bearing the UAS-MJDtr-Q27, UAS-MJDtr-Q78, UAS-Htt-Q128, or *gmr*-GAL4 transgene have been described previously (27, 28). The transgenic fly line bearing the *elav*-GAL4 transgene was obtained from the Bloomington *Drosophila* Stock Center. The MJDtr-Q27 and MJDtr-Q78 fly lines express a truncated form of the MJD protein with the indicated number of glutamines (MJDtr-Q27 and MJDtr-Q78 proteins, respectively), and the Htt-Q128 fly line expresses an N-terminal fragment of the huntingtin protein with 128 glutamines (Htt-Q128 protein), under the control of the GAL4-UAS system. For the MJDtr-Q78 flies, the W line showing weak and the S line showing strong phenotypes were used (27). The chemical compounds to be tested were dissolved in ethanol, further diluted in water, and then mixed with Instant *Drosophila* medium (Carolina Biological Supply Company, Burlington, NC). 17-AAG was purchased from Biomol Research Laboratories (Plymouth Meeting, PA); geldanamycin (GA) and radicicol (RA) were from Sigma-Aldrich; celastrol (CL) was from Merck; and sodium butyrate (SB) was from Nacalai Tesque (Kyoto, Japan). Geranylgeranylacetone (GGA) supplemented with 0.2% α-tocopherol was kindly provided by Eisai Co. (Tokyo, Japan). These compounds were used for flies at the following concentrations: 17-AAG, GA, and RA (50 nM, 500 nM, 5 μM, and 50 μM); CL (1 μM, 10 μM, and 100 μM); SB (10 mM); and GGA (1 nM, 10 nM, 100 nM, and 40 mM). These compounds at the above concentrations did not affect the viability and fertility of the MJDtr-Q78 flies. For heat shock treatment, crawling third instar larvae were incubated at 37 °C for 15 min and recovered at 25 °C for 1 h.

*Microscopy, Histology, and Immunohistochemistry*—To evaluate the therapeutic effects of HSF1-activating compounds on compound eye degeneration in the MJDtr-Q78S flies, light microscopic images of the compound eye morphologies of 1-day-old adult flies were taken using a stereoscopic microscope model SZX9 (Olympus, Tokyo, Japan). To assess the therapeutic effects of HSF1-activating compounds on photoreceptor degeneration in the Htt-Q128 flies, heads of 1-day-old Htt-Q128 flies treated with 17-AAG, GA, or RA (5 μM) were fixed in 2% paraformaldehyde and 2.5% glutaraldehyde and embedded in Epon. Compound eyes were sectioned at 1 μm and stained with 0.5% toluidine blue. Microscopic images were

taken using a fluorescence microscope model DMR (Leica Microsystems, Wetzlar, Germany) with a CCD camera model DC500 (Leica Microsystems), and the average number of rhabdomeres/ommatidium was calculated. The percentage of rescue of photoreceptor degeneration was calculated by dividing the difference in the number of rhabdomeres between the 17-AAG-treated and untreated Htt-Q128 flies by the decrease in the number of rhabdomeres in the untreated Htt-Q128 flies. The number of rhabdomeres/ommatidium was counted in 20 ommatidia/fly, and at least 100 ommatidia were assessed for each condition except for SB treatment (60 ommatidia). The data are expressed as the means ± S.E.

For immunohistochemical analysis, eye discs of the MJDtr-Q78W flies treated with 17-AAG (1.5 μM) were dissected from crawling third instar larvae and fixed in 4% paraformaldehyde. The eye discs were immunostained with a rat monoclonal anti-hemagglutinin (HA) antibody (clone 3F10; Roche Applied Science) at 1:100 dilution as the primary antibody to detect the MJDtr-Q78 protein and Alexa 546-conjugated anti-rat IgG antibody (Invitrogen) at 1:2000 dilution as the secondary antibody. The images were taken using a confocal laser scanning microscope model LSM510 (Carl Zeiss, Oberkochen, Germany). The anteroposterior width of the eye disc area with cells containing inclusion bodies of the MJDtr-Q78 protein (Wi; see Fig. 5*F*) and that of the area with cells containing the diffusely distributed MJDtr-Q78 protein (Wd; see Fig. 5*F*) were measured using National Institutes of Health Image software. The ratio of Wi/Wd in each eye disc was calculated to evaluate the degree of inclusion body formation. At least seven discs were analyzed for each treatment condition. The data are expressed as the means ± S.E.

*Fly Survival Analyses*—To examine the therapeutic effects of 17-AAG on the survival rate during development to adults of flies expressing the MJDtr-Q78 protein in the nervous system, we crossed flies homozygous for the UAS-MJDtr-Q78S transgene with flies bearing the *elav*-Gal4 driver transgene in trans to the balancer chromosome (CyO). 50% of the progeny are expected to bear both the *elav*-Gal4 driver and the UAS-MJDtr-Q78S transgenes (MJDtr-Q78S flies), which express the MJDtr-Q78 protein, whereas 50% of the progeny are expected to bear the UAS-MJDtr-Q78S transgene and CyO (control flies), which do not express the MJDtr-Q78 protein. The ratio of the MJDtr-Q78S flies to the control flies was calculated by dividing the number of emerging flies not bearing CyO (MJDtr-Q78S flies) by that of emerging flies bearing CyO (control flies) to evaluate the survival rate of the MJDtr-Q78S flies during their development to adults. The percentage of rescue of the lethality was calculated by dividing the difference in the survival rate between the 17-AAG-treated and untreated MJDtr-Q78S flies by the decrease in the survival rate of the untreated MJDtr-Q78S flies. At least 100 flies were scored for each treatment condition, and the experiments were repeated three times. The data are expressed as the means ± S.E.

*Western Blot Analyses*—To assess the effect of 17-AAG on the expression level of the MJDtr-Q78 protein, 10 heads of the MJDtr-Q78S flies treated with 17-AAG (5 μM) were lysed in 100 μl of Laemmli sample buffer and then centrifuged at 17,000 × *g* for 10 min at 25 °C. The resultant supernatants were separated on a 10% polyacrylamide gel and then transferred onto Immobilon-P membranes (Millipore, Billerica, MA). The membranes were incubated overnight with either a rat monoclonal anti-HA antibody (clone 3F10; Roche Applied Science) at 1:2000 dilution to detect the MJDtr-Q78 protein or a sheep polyclonal anti-tubulin antibody (Cytoskeleton Inc., Denver, CO) at 1:4000 dilution. Horseradish peroxidase (HRP)-conjugated rabbit anti-rat Igs antibody (DakoCytomation, Glostrup, Denmark) or HRP-conjugated rabbit anti-sheep Igs antibody (DakoCytomation) were used at 1:5000 dilution as secondary antibodies. To detect the HSF1 protein in transfected Schneider line 2 (SL2) cell lysates, a mouse monoclonal anti-Myc antibody (clone 9E10; Invitrogen; 1:2000 dilution) and HRP-conjugated rabbit anti-mouse Igs antibody (DakoCytomation; 1:5000 dilution) were used. The HRP was detected using SuperSignal West Pico Chemiluminescent Substrate (Pierce).

*RT-PCR Analyses*—Total RNA was purified from whole bodies or eye-antennal discs of crawling third instar larvae of the MJDtr-Q78S flies and control flies expressing the GAL4 activator protein alone using the RNeasy Mini Kit (Qiagen) according to the manufacturer's instructions and was reverse transcribed with random hexamer primers. We performed PCR analyses of Hsp70, Hsp40, and Hsp90 mRNAs with the following primers: Hsp70-F, 5′-AGCCGTGCCAGGTTTG-3′ and Hsp70-R, 5′-CGTTCGCCCTCATACA-3′; Hsp40-F, 5′-CATAAAGCAGCCCGTGTAGC-3′ and Hsp40-R, 5′-AGATGTTGAGGCACCGATTC-3′; and Hsp90-F, 5′-CGATTAAGCGACCAGTCGAA-3′ and Hsp90-R, 5′-AAACGACAACTGCTCTTGAATG-3′. As an internal control, mRNA of rp49 (ribosomal protein 49), a housekeeping gene, was also analyzed with the primers rp49-F, 5′-AGCGCACCAAGCACTTCATCCGCCA-3′ and rp49-R, 5′-GCGCACGTTGTGCACCAGGAACTTC-3′. The RT-PCR products were separated on a 3% agarose gel and visualized by ethidium bromide staining. For precise quantification, real time quantitative PCR was performed with the above primers and Premix Ex Taq (Takara, Shiga, Japan) using ABI PRISM 7900 HT (Applied Biosystems, Foster City, CA). The relative abundance of each mRNA was calculated by normalizing to rp49 mRNA according to the manufacturer's instructions. To compare the expression levels of each mRNA, the ratio of each mRNA/rp49 mRNA of the 17-AAG-treated MJDtr-Q78S flies expressing the MJDtr-Q78 protein alone or co-expressing the HSF1 RNAi was divided by that of the untreated MJDtr-Q78S flies. The experiments were repeated at least three times. The data are expressed as the means ± S.E.

*Vector Construction and Generation of Transgenic Fly Lines*—For expression of the HSF1 protein, a DNA fragment coding for dHSFa, the major alternatively spliced isoform of *Drosophila* HSF1 (21), tagged with a c-Myc epitope was inserted into the pUAST vector, to generate the pUAS-HSF1 vector. For the HSF1 knockdown experiment, the pUAS-HSF1-RNAi vector harboring inverted repeats corresponding to the third to fifth exon of the HSF1 cDNA separated by the second intron of the HSF1 gene was constructed according to the strategy for splice activated RNAi. To establish HSF1 RNAi fly lines, the pUAS-HSF1-RNAi vector was injected into fly embryos by standard procedures.

*Cell Culture and Transfection*—SL2 cells, which were derived from late stage fly embryos, were cultured in Schneider's insect medium (Sigma-Aldrich) supplemented with 10% fetal calf serum at 25 °C. To evaluate the efficiency of RNAi-mediated HSF1 knockdown, SL2 cells were co-transfected with the pUAS-HSF1 vector along with either the pUAS-HSF1-RNAi or pUAST empty vector, as well as the pAct5C-GAL4 vector as a driver using Effectene transfection reagent (Qiagen) according to the manufacturer's instructions. The cells were harvested 48 h after transfection, and the cell lysates were subjected to Western blot analyses.

## RESULTS

*17-AAG Treatment Suppresses polyQ-induced Neurodegeneration in Drosophila*—To evaluate the therapeutic effects of HSF1-activating compounds, which induce multiple endogenous molecular chaperones, on polyQ-induced neurodegeneration, we chose the following five compounds. GA, a benzoquinone ansamycin anti-tumor antibiotic, specifically inhibits the activity of Hsp90, a negative regulator of HSF1, resulting in activation of HSF1 (18). 17-AAG, a derivative of GA, shares the property to inhibit Hsp90 but has less cytotoxicity than GA (29). RA, an antifungal macrolactone antibiotic, also inhibits the activity of Hsp90 (30). CL, a potent anti-inflammatory compound, activates HSF1 through unknown mechanisms (31). GGA, an anti-ulcer agent, activates protein kinase C, leading to the phosphorylation and activation of HSF1 (26). We employed *Drosophila* polyQ disease models to analyze the therapeutic effects of oral administration of the above compounds, because *Drosophila melanogaster* has been shown to be a useful *in vivo* model to study polyQ-induced neurodegeneration (27, 28). We administered the above HSF1-activating compounds by mixing them in culture food to the transgenic fly line MJDtr-Q78S, which expresses the MJDtr-Q78 protein in the eye under the *gmr* promoter, resulting in severe compound eye degeneration (27).

Treatment with the HSF1-activating compounds revealed that 17-AAG is most effective against polyQ-induced compound eye degeneration (Figs. 1 and 2). 17-AAG treatment at concentrations of 500 nM, 1.5 μM, and 5 μM strongly suppressed polyQ-induced compound eye degeneration (Fig. 2, *C–E*), whereas treatment at 50 nM showed a moderate therapeutic effect (Fig. 2*B*). However, 17-AAG treatment at 50 μM unexpectedly failed to improve compound eye degeneration in the MJDtr-Q78S flies (Fig. 2*F*), indicating that the therapeutic effect of 17-AAG is dose-dependent at least up to 5 μM. Treatment with GA at concentrations of 500 nM and 5 μM also showed modest suppression of polyQ-induced compound eye degeneration (Fig. 1*C*), whereas treatment at 50 nM and 50 μM did not (data not shown). Treatment with RA at concentrations ranging from 50 nM to 5 μM was also effective against polyQ-induced compound eye degeneration (Fig. 1*D*). However, treatment with either CL (1 to 100 μM) or GGA (10 μM to 40 mM) did not show any detectable changes (Fig. 1, *E* and *F*). Compared with the therapeutic effects of SB, a histone deacetylase inhibitor, which was previously reported to suppress polyQ-induced neurodegeneration (7), 17-AAG showed a remarkably greater

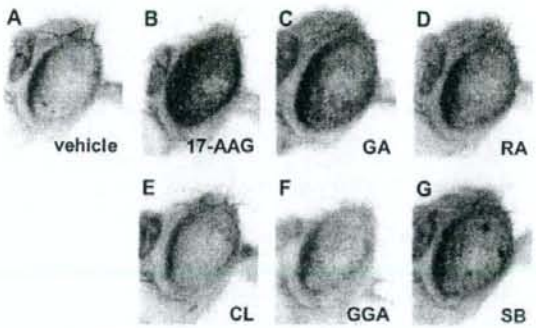


FIGURE 1. **17-AAG treatment suppresses compound eye degeneration in the MJDtr-Q78S flies.** Light microscopic images of the compound eye morphologies of 1-day-old MJDtr-Q78S flies treated with various HSF1-activating compounds. *A*, untreated MJDtr-Q78S flies show severe compound eye degeneration. *B*, notably, treatment with 17-AAG (1.5 μM), an HSF1-activating compound, strongly suppressed compound eye degeneration in the MJDtr-Q78S flies. *C* and *D*, treatment with GA (5 μM, *C*) or RA (5 μM, *D*) moderately suppressed compound eye degeneration. *E* and *F*, treatment with neither CL (100 μM, *E*) nor GGA (40 mM, *F*) showed any detectable changes in compound eye degeneration. *G*, treatment with SB (10 mM), a histone deacetylase inhibitor used as a positive control, weakly suppressed compound eye degeneration. Fly genotype is *gmr*-GAL4/+; UAS-MJDtr-Q78S/+.

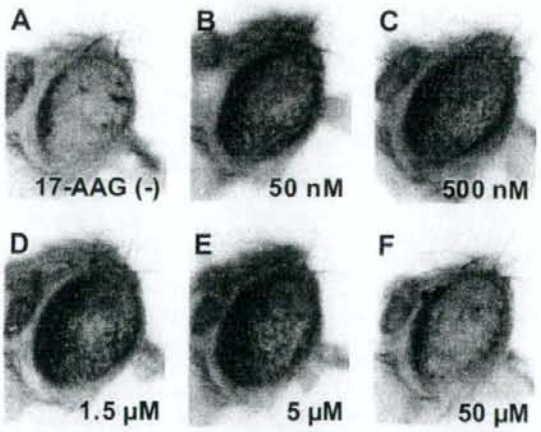


FIGURE 2. **17-AAG suppresses polyQ-induced compound eye degeneration in a dose-dependent manner.** Light microscopic images of the compound eye morphologies of 1-day-old MJDtr-Q78S flies treated with various concentrations of 17-AAG. *A*, untreated MJDtr-Q78S flies. *B–F*, 17-AAG treatment at concentrations of 500 nM (*C*), 1.5 μM (*D*), and 5 μM (*E*) strongly suppressed compound eye degeneration in the MJDtr-Q78S flies, whereas treatment at 50 nM (*B*) showed modest suppression. However, 17-AAG treatment at 50 μM (*F*) failed to improve compound eye degeneration in the MJDtr-Q78S flies. These data indicate that 17-AAG treatment up to 5 μM suppresses polyQ-induced neurodegeneration in a dose-dependent manner. Fly genotype is *gmr*-GAL4/+; UAS-MJDtr-Q78S/+.

improvement of polyQ-induced compound eye degeneration (Fig. 1, *B* and *G*).

To examine whether HSF1-activating compounds are widely effective against various polyQ diseases, we administered 17-AAG, GA, and RA to the transgenic fly line Htt-Q128, which expresses the Htt-Q128 protein in the eye under the *gmr* promoter, resulting in progressive photoreceptor degeneration (28). The loss of photoreceptor neurons in the Htt-Q128 flies can be quantitatively evaluated as a decrease in the number of

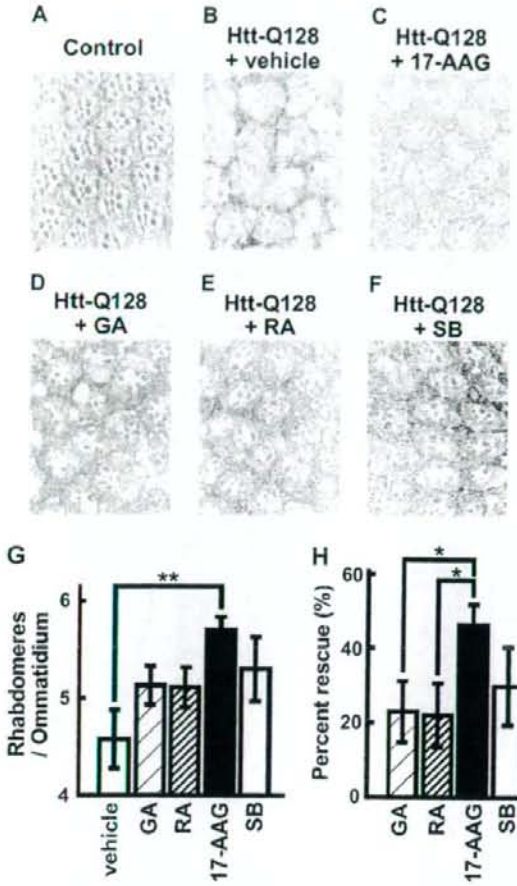


FIGURE 3. **17-AAG suppresses degeneration of photoreceptor neurons in the Htt-Q128 flies.** *A–F*, toluidine blue-stained sections of the eyes of 1-day-old Htt-Q128 flies treated with various HSF1-activating compounds (5 $\mu$M). Expression of the Htt-Q128 protein caused progressive photoreceptor degeneration, resulting in loss of rhabdomeres in each ommatidium (*B*), whereas flies expressing the GAL4 activator protein alone (*Control*) showed normal structures of ommatidia (*A*). Notably, 17-AAG remarkably suppressed photoreceptor degeneration in the Htt-Q128 flies (*C*). GA (*D*) and RA (*E*) moderately suppressed photoreceptor degeneration. SB, used as a positive control, also showed moderate suppression (*F*). Fly genotypes are *gmr*-GAL4/+; UAS-Htt-Q128/+ (*B–F*) or *gmr*-GAL4/+ (*A*). *G*, the average number of rhabdomeres/ommatidium in the Htt-Q128 flies treated with various HSF1-activating compounds. 17-AAG significantly suppressed photoreceptor degeneration, resulting in an increase in the number of rhabdomeres/ommatidium from 4.6 ± 0.3 to 5.7 ± 0.1. GA, RA, and SB modestly increased the number of rhabdomeres to 5.1 ± 0.2, to 5.1 ± 0.2, and to 5.3 ± 0.3, respectively. *H*, the percentage of rescue of photoreceptor degeneration in the Htt-Q128 flies by treatment with HSF1-activating compounds. 17-AAG most effectively rescued photoreceptor degeneration in the Htt-Q128 flies (46.3 ± 5.5%) as compared with GA, RA, and SB (22.8 ± 8.3, 22.0 ± 8.5, and 29.8 ± 10.5% respectively). The data are expressed as the means ± S.E. ($n \geq 3$). *, $p < 0.05$; **, $p < 0.01$ (Student's *t* test).

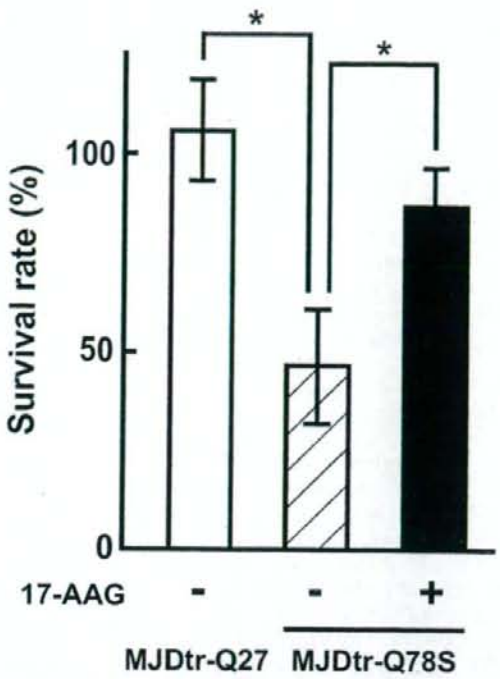


FIGURE 4. **17-AAG increases the survival rate of the MJDtr-Q78S flies during their development to adults.** The survival rates during the development to adults are shown of flies expressing the MJDtr-Q78 protein within the nervous system treated with 17-AAG. The ratio of the MJDtr-Q78S flies to the control flies was calculated by dividing the number of emerging flies not bearing CyO (MJDtr-Q78S flies) by that of emerging flies bearing CyO (control flies) to evaluate the survival rate of the MJDtr-Q78S flies. Expression of the MJDtr-Q78 protein significantly decreased the survival rate (46.2 ± 14.4%), whereas the MJDtr-Q27 protein did not cause any significant changes (105.2 ± 12.6%). Notably, 17-AAG treatment significantly increased the survival rate of the MJDtr-Q78S flies (86.0 ± 9.8%), corresponding to a 74.1 ± 16.5% rescue of the lethality. The data are expressed as the means ± S.E. ($n = 3$). *, $p < 0.05$ (Student's *t* test). Fly genotypes are *elav*-GAL4/UAS-MJDtr-Q78S (MJDtr-Q78S) or *elav*-GAL4/UAS-MJDtr-Q27 (MJDtr-Q27).

rhabdomeres in each ommatidium (Fig. 3, *B* and *G*), which normally has seven rhabdomeres (Fig. 3*A*). We found that 17-AAG treatment markedly suppresses photoreceptor degeneration, resulting in an increase in the number of rhabdomeres/ommatidium from 4.6 ± 0.3 to 5.7 ± 0.1 in the Htt-Q128 flies (Fig. 3, *C* and *G*), corresponding to a 46.3 ± 5.5% rescue (Fig. 3*H*). Treatment with GA and RA modestly increased the number of rhabdomeres in the Htt-Q128 flies to 5.1 ± 0.2 (22.8 ± 8.3% rescue) and to 5.1 ± 0.2 (22.0 ± 8.5% rescue), respectively (Fig. 3, *D*, *E*, *G*, and *H*), which were similar levels to SB treatment (29.8 ± 10.5% rescue) (Fig. 3, *F–H*), although the suppression was not statistically significant. Among the HSF1-activating compounds tested, 17-AAG was the most effective against photoreceptor degeneration in the Htt-Q128 flies (Fig. 3*H*), consistent with their therapeutic effects in the MJDtr-Q78S flies (Fig. 1). These data indicate that 17-AAG widely suppresses eye degeneration induced by various polyQ proteins.

We next examined whether 17-AAG suppresses polyQ-induced neurodegeneration broadly within the nervous system, because various regions of the nervous system are widely affected in human patients. Expression of the MJDtr-Q78 protein within the nervous system under the *elav* promoter significantly decreased the survival rate of flies during their development to adults, because of neurodegeneration (46.2 ± 14.4%; Fig. 4), whereas expression of the MJDtr-Q27 protein, which has a nor-

mal-length polyQ stretch, did not cause any significant changes (105.2 ± 12.6%). We found that 17-AAG treatment significantly increases the survival rate of the MJDtr-Q78S flies (86.0 ± 9.8%; Fig. 4), corresponding to a 74.1 ± 16.5% rescue of the lethality. These data indicate that 17-AAG is effective against polyQ-induced neurodegeneration broadly within the nervous system, and its efficiency is not limited to compound eye degeneration. We therefore conclude that 17-AAG, an HSF1-activating compound, is effective against neurodegeneration in *Drosophila* models of various polyQ diseases.

*17-AAG Suppresses Inclusion Body Formation of the polyQ Protein without Affecting Its Expression Level*—To evaluate the effect of 17-AAG on misfolding of the polyQ protein, we examined polyQ inclusion body formation upon 17-AAG treatment in a *Drosophila* polyQ disease model. Misfolded polyQ proteins are known to form aggregates and to eventually accumulate as inclusion bodies not only in human patients but also in *Drosophila* models (27, 28). Immunostaining of the eye discs of the MJDtr-Q78W fly larvae, which express the MJDtr-Q78 protein under the *gmr* promoter, revealed numerous inclusion bodies (Fig. 5*A*, *arrows*) in the region posterior to the morphogenetic furrow (*arrowhead*), as reported previously (27). We found that the MJDtr-Q78W flies treated with 17-AAG have significantly fewer inclusion bodies as compared with the untreated flies (Fig. 5, *A* and *B*, *arrows*). Upon higher magnification, the number and sizes of inclusion bodies in the MJDtr-Q78W flies were clearly reduced by 17-AAG treatment (Fig. 5, *C* and *D*), suggesting that 17-AAG suppresses polyQ inclusion body formation. For quantification of the effect of 17-AAG on inclusion body formation, we evaluated the anteroposterior width of the eye disc area with cells containing inclusion bodies (Fig. 5*F*, *Wi*). The ratio of the area with inclusions to the area with diffuse distribution of the MJDtr-Q78 protein (Wi/Wd) has been shown to gradually increase with disease progression (32), because terminal differentiation of cells and hence expression of the protein begin in the posterior end of the eye discs and spread toward the anterior. We found that 17-AAG treatment significantly decreases the Wi/Wd ratio in the eye discs of the MJDtr-Q78W flies from 0.84 ± 0.04 to 0.59 ± 0.05 (Fig. 5*E*). These data indicate that 17-AAG delays inclusion body formation of the MJDtr-Q78 protein. In addition, the intensity of the diffusely distributed MJDtr-Q78 protein in the 17-AAG-treated MJDtr-Q78W flies was similar to that in untreated flies (Fig. 5, *A* and *B*), suggesting that the delay in inclusion body formation by 17-AAG treatment is not due to a reduction in the expression level of the MJDtr-Q78 protein.

To further confirm that 17-AAG treatment does not affect the polyQ protein expression level, we evaluated MJDtr-Q78 protein expression by Western blot. We found that the expression level of the MJDtr-Q78 protein in the 17-AAG-treated MJDtr-Q78S flies was similar to that in untreated flies (Fig. 5*G*). These data suggest that 17-AAG suppresses polyQ inclusion body formation by suppression of protein misfolding rather than by the reduction of the polyQ protein expression level.

*Therapeutic Effects of 17-AAG on polyQ-induced Neurodegeneration Correlate with the Induction Levels of Molecular Chaperones*—To confirm whether the therapeutic effects of 17-AAG on polyQ-induced neurodegeneration depend on

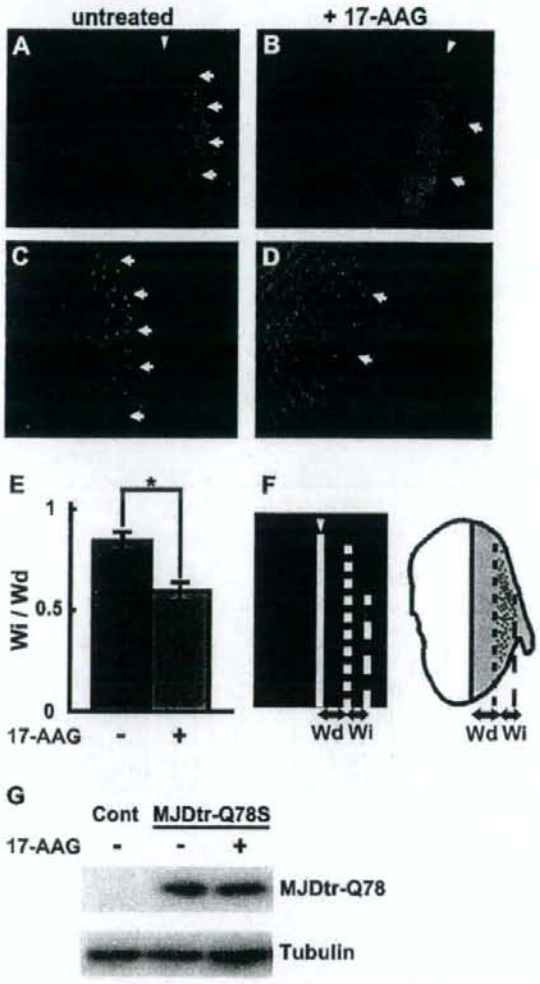


FIGURE 5. **17-AAG suppresses inclusion body formation of the MJDtr-Q78 protein without affecting its expression level.** *A–D*, confocal microscopic images of eye-antennal discs of third instar larvae of the MJDtr-Q78W flies treated with 17-AAG (1.5 μM), stained with an anti-HA antibody to detect the MJDtr-Q78 protein. Lower (×200, A, B) and higher (×630, C, D) magnification images are shown. Eye portions (posterior) are to the *right*, and antennal portions (anterior) to the *left*. The *arrowheads* indicate morphogenetic furrows. The 17-AAG-treated MJDtr-Q78W flies (*B* and *D*) have significantly fewer inclusion bodies (*arrows*) as compared with the untreated flies (*A* and *C*). *E* and *F*, quantitative analyses of the effects of 17-AAG on inclusion body formation. Schematic representation is shown of an eye disc, in which inclusion bodies (*red*) are formed in the area where the MJDtr-Q78 protein is expressed (*gray* in *F*, *right*). The ratio of the anteroposterior width of the area with cells containing inclusion bodies (*Wi*) to that of the area with cells containing the diffusely distributed MJDtr-Q78 protein (*Wd*) was calculated. The ratio of Wi/Wd was significantly decreased by 17-AAG treatment from 0.84 ± 0.04 to 0.59 ± 0.05 (*E*). The data are expressed as the means ± S.E. ($n \geq 7$). *, $p < 0.01$ (Student's *t* test). Fly genotype is *gmr*-GAL4/+; +; UAS-MJDtr-Q78W/+. *G*, Western blot analyses of the MJDtr-Q78 protein in the MJDtr-Q78S flies treated with 17-AAG using an anti-HA antibody to detect the MJDtr-Q78 protein (*upper panel*) and an anti-tubulin antibody (*lower panel*). 17-AAG did not affect the expression level of the MJDtr-Q78 protein. Fly genotypes are *gmr*-GAL4/+, UAS-MJDtr-Q78S/+ (MJDtr-Q78S), or *gmr*-GAL4/+ (control, *Cont*).

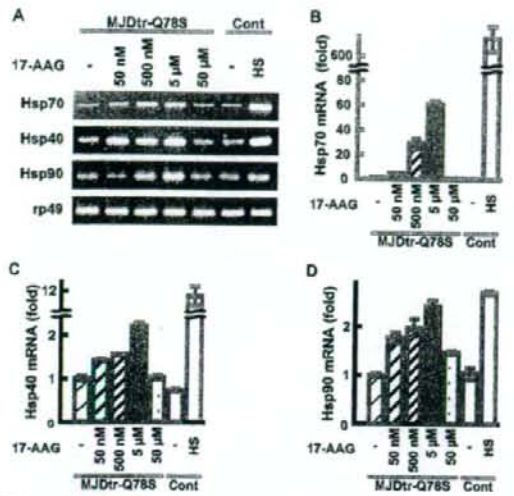


FIGURE 6. **17-AAG induces expression of molecular chaperones in a dose-dependent manner.** *A*, RT-PCR analyses of Hsp70, Hsp40, and Hsp90 mRNAs expressed in third instar larvae of the MJDtr-Q78S flies treated with 17-AAG (50 nM, 500 nM, 5 μM, or 50 μM). Flies expressing the GAL4 activator protein alone (*Cont*) exposed to heat shock (*HS*) were used as a positive control. The rp49 mRNA was also analyzed as an internal control. *B–D*, real time quantitative RT-PCR analyses of Hsp70, Hsp40, and Hsp90 mRNAs expressed in the MJDtr-Q78S fly larvae. Treatment with 17-AAG up to 5 μM induced expression of Hsp70 (*B*), Hsp40 (*C*), and Hsp90 (*D*) mRNAs in a dose-dependent manner (60.87-, 2.20-, and 2.42-fold at 5 μM, respectively). The results shown are from representative experiments. The data are expressed as the means ± S.E. ($n = 3$). Fly genotypes are *gmr*-GAL4/+, UAS-MJDtr-Q78S/+ (MJDtr-Q78S), or *gmr*-GAL4/+ (control).

induction of molecular chaperones, we assessed their expression levels upon 17-AAG treatment. We examined the expression levels of Hsp70, Hsp40, and Hsp90 mRNAs in the 17-AAG-treated MJDtr-Q78S fly larvae by RT-PCR analyses, because these molecular chaperones are reported to suppress polyQ-induced cytotoxicity (11, 12, 16). We found that 17-AAG treatment up to 5 μM induces expression of Hsp70, Hsp40, and Hsp90 mRNAs in the MJDtr-Q78S flies, whereas treatment at 50 μM does not (Fig. 6*A*). For precise quantification of the increases in the mRNA levels of these Hsps, we performed real time quantitative RT-PCR analyses. We found that the expression levels of Hsp70 mRNA in the MJDtr-Q78S flies are significantly increased by 17-AAG treatment at concentrations ranging from 50 nM to 5 μM in a dose-dependent manner (50 nM, 4.53-fold; 500 nM, 29.04-fold; and 5 μM, 60.87-fold; Fig. 6*B*), although the levels of induction are not as robust as heat shock treatment (Fig. 6*B*, *HS*). However, 17-AAG treatment at 50 μM did not induce expression of Hsp70 mRNA at all (0.64-fold), which is consistent with the lack of a therapeutic effect on polyQ-induced neurodegeneration (Fig. 2*F*). We also found that 17-AAG treatment up to 5 μM induced expression of Hsp40 mRNA in a dose-dependent manner (50 nM, 1.41-fold; 500 nM, 1.53-fold; and 5 μM, 2.20-fold; Fig. 6*C*), whereas treatment at 50 μM did not. The expression levels of Hsp90 mRNA were also increased by 17-AAG treatment up to 5 μM in a dose-dependent manner (50 nM, 1.77-fold; 500 nM, 1.98-fold; and 5 μM, 2.42-fold; Fig. 6*D*) and were similar to that upon heat shock treatment (2.71-fold; Fig. 6*D*). 17-AAG treatment at 50 μM slightly induced expression of Hsp90 mRNA (1.47-fold). Taken together, we conclude that 17-AAG treatment up to 5 μM induces multiple molecular chaperones in a dose-dependent manner and that their expression levels correlate with the therapeutic effects of 17-AAG on polyQ-induced neurodegeneration.

*Therapeutic Effects of 17-AAG on polyQ-induced Neurodegeneration Are Mediated by HSF1 Activation*—We next determined whether the therapeutic effects of 17-AAG on polyQ-induced neurodegeneration through induction of multiple molecular chaperones are mediated by HSF1 activation. For this purpose, we examined whether RNAi-mediated knockdown of endogenous HSF1 affects the therapeutic effects of 17-AAG on the MJDtr-Q78S flies. We first designed a double-stranded RNA construct against HSF1 (HSF1 RNAi) and evaluated its efficiency of HSF1 knockdown in *Drosophila* SL2 cells. SL2 cells were co-transfected with expression vectors for the HSF1 protein and HSF1 RNAi, and the cell lysates were subjected to Western blot analysis. In the cells transfected with the HSF1 vector alone, we found that the HSF1 band appears as a doublet, probably because of phosphorylation, as reported previously (Fig. 7*A*, *middle lane*). In contrast, the HSF1 protein was hardly detected in the cells co-transfected with the HSF1 vector and the HSF1 RNAi vector (Fig. 7*A*, *right lane*), indicating that this HSF1 RNAi construct almost completely knocks down expression of the HSF1 protein. Accordingly, we established transgenic HSF1 RNAi flies expressing this HSF1 RNAi construct under the *gmr* promoter and confirmed that these flies do not show any detectable phenotypes in their compound eyes (data not shown). We then crossed these HSF1 RNAi flies with the MJDtr-Q78S flies to evaluate the effects of HSF1 knockdown on 17-AAG treatment. Notably, knockdown of endogenous HSF1 almost completely abolished the therapeutic effect of 17-AAG on compound eye degeneration in the MJDtr-Q78S flies (Fig. 7, *D* and *E*). The level of compound eye degeneration in the 17-AAG-treated MJDtr-Q78S flies co-expressing the HSF1 RNAi was similar to that in the untreated MJDtr-Q78S flies (Fig. 7, *B* and *E*). These data indicate that endogenous HSF1 is essential for the therapeutic effects of 17-AAG on polyQ-induced neurodegeneration. However, we cannot exclude the possibility that knockdown of HSF1 simply masks the therapeutic effects of 17-AAG independently of affecting the induction of molecular chaperones, because HSF1 knockdown itself slightly enhances polyQ-induced compound eye degeneration in the MJDtr-Q78S flies (Fig. 7*C*), consistent with a previous report (33).

To further confirm whether the therapeutic effects of 17-AAG depend on HSF1-mediated induction of molecular chaperones, we examined the expression level of Hsp70 mRNA in the 17-AAG-treated MJDtr-Q78S flies co-expressing the HSF1 RNAi. We performed quantitative RT-PCR analyses using eye-antennal discs of the fly larvae, because the HSF1 RNAi construct is expressed only in the eye discs under the *gmr* promoter. We confirmed that 17-AAG treatment significantly induces expression of Hsp70 mRNA in the eye-antennal discs of the MJDtr-Q78S fly larvae (2.37-fold; Fig. 7*F*) as was observed in their whole bodies (Fig. 6). Notably, knockdown of endogenous HSF1 dramatically decreased the expression level of

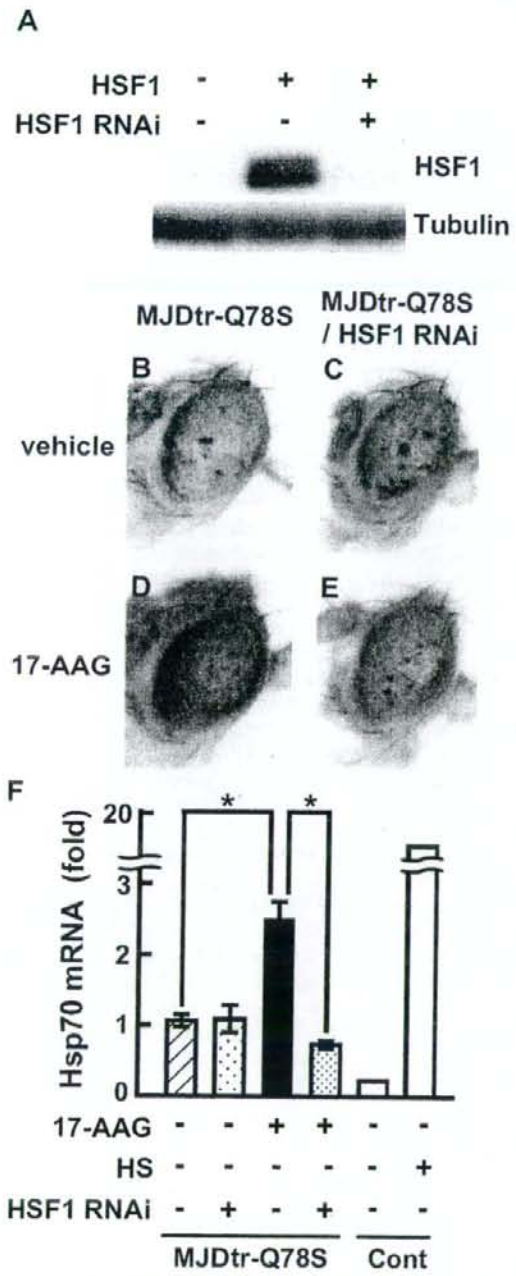


FIGURE 7. **RNAi-mediated knockdown of HSF1 abolishes the therapeutic effect of 17-AAG on compound eye degeneration in the MJDtr-Q78S flies.** *A*, Western blot analyses of the HSF1 protein expressed in SL2 cells co-transfected with expression vectors for the HSF1 protein and HSF1 RNAi, using the anti-Myc antibody to detect the HSF1 protein (*upper panel*) and the anti-tubulin antibody (*lower panel*). Co-expression of the HSF1 RNAi almost completely knocks down expression of the HSF1 protein. *B–E*, light microscopic images of the compound eye morphologies of the 17-AAG (5 $\mu$M)-treated MJDtr-Q78S flies expressing the MJDtr-Q78 protein alone (*D*) or co-expressing the HSF1 RNAi (*E*). Untreated MJDtr-Q78S flies expressing the MJDtr-Q78 protein alone (*B*) or co-expressing the HSF1 RNAi (*C*) are also shown. Co-expression of the HSF1 RNAi almost completely abolished the therapeutic effect of 17-AAG on compound eye degeneration in the MJDtr-Q78S flies. Fly genotypes are *gmr*-GAL4/+, UAS-MJDtr-Q78S/+, +/+ (*B* and *D*) or *gmr*-GAL4/+, UAS-MJDtr-Q78S/+, and UAS-HSF1-RNAi/+ (*C* and *E*). *F*, real time quantitative RT-PCR analyses of Hsp70 mRNA expressed in the eye-antennal discs of the 17-AAG (5 $\mu$M)-treated MJDtr-Q78S fly larvae co-expressing the HSF1 RNAi or expressing the MJDtr-Q78 protein alone. Flies expressing the GAL4 activator protein alone (control, *Cont*) exposed to heat shock (*HS*) were used as a positive control. Co-expression of the HSF1 RNAi decreased the expression level of Hsp70 mRNA in the 17-AAG-treated MJDtr-Q78S fly larvae from 2.37- to 0.68-fold. The experiments were repeated at least four times except for control flies. The results from representative experiments are shown for control flies. The data are expressed as the means ± S.E. ($n \geq 3$). *, $p < 0.01$ (Student's *t* test). Fly genotypes are *gmr*-GAL4/+, UAS-MJDtr-Q78S/+ (MJDtr-Q78S), *gmr*-GAL4/+, UAS-MJDtr-Q78S/UAS-HSF1-RNAi (MJDtr-Q78S/HSF1 RNAi), or *gmr*-GAL4/+ (Cont).

Hsp70 mRNA in the 17-AAG-treated MJDtr-Q78S fly larvae (0.68-fold; Fig. 7*F*), which was similar to that in the untreated MJDtr-Q78S flies. These data indicate that endogenous HSF1 is required for induction of molecular chaperones by 17-AAG treatment, and we therefore conclude that the therapeutic effects of 17-AAG on polyQ-induced neurodegeneration depend on HSF1-mediated induction of molecular chaperones.

## DISCUSSION

Recently, many neurodegenerative diseases including Alzheimer disease, Parkinson disease, amyotrophic lateral sclerosis, and the polyQ diseases are thought to be caused by protein misfolding, and hence suppression of protein misfolding by molecular chaperones is considered to be a common therapeutic approach for these neurodegenerative diseases (14). In fact, genetic expression of Hsp70, a molecular chaperone, has been shown to suppress neurodegeneration in cell culture and animal models of Parkinson disease, amyotrophic lateral sclerosis, and the polyQ diseases (34–36). Furthermore, induction of multiple molecular chaperones including Hsp70 and Hsp40 by genetic expression of a constitutively active mutant of HSF1 has been shown to be more effective against amyotrophic lateral sclerosis and the polyQ diseases compared with expression of Hsp70 alone (24, 37). As a next step toward developing a therapy, we evaluated the therapeutic effects of pharmacological induction of multiple endogenous molecular chaperones by HSF1-activating compounds in *Drosophila* models of the polyQ diseases. In this study, we show that 17-AAG treatment successfully suppresses neurodegeneration through induction of Hsp70, Hsp40 and Hsp90 in a *Drosophila* model of SCA3/MJD, one of the polyQ diseases (Figs. 1, 2, 4, and 6). 17-AAG also significantly suppressed neurodegeneration in a model of Huntington disease, another polyQ disease (Fig. 3), indicating that 17-AAG is widely effective against various polyQ diseases. In addition, 17-AAG clearly reduced inclusion bodies composed of misfolded polyQ proteins (Fig. 5), consistent with previous reports showing that co-expression of Hsp70 together with Hsp40 synergistically suppresses polyQ inclusion body formation (8, 38). Moreover, induction of Hsp70 by GA treatment has been reported to suppress neurodegeneration in a *Drosophila* model of Parkinson disease (39). Induction of molecular chaperones by treatment with arimoclomol, which is also known to activate HSF1, has been reported to suppress neurodegeneration in a mouse model of amyotrophic lateral

sclerosis (40). Therefore, treatment with HSF1-activating compounds to induce multiple endogenous molecular chaperones is a promising therapeutic approach for the polyQ diseases as well as other neurodegenerative diseases.

We show that 17-AAG is the most effective agent against polyQ-induced neurodegeneration in *Drosophila* among the HSF1-activating compounds we studied (Fig. 1). In addition to 17-AAG, GA, and RA also showed weaker suppression of polyQ-induced neurodegeneration, consistent with previous reports showing that GA and RA suppress polyQ protein misfolding *in vitro* (41). On the other hand, GGA was not effective against polyQ-induced neurodegeneration in this study, although it has been reported to mitigate the neurological phenotypes of a mouse model of spinobulbar muscular atrophy (42). GGA has recently been demonstrated to activate HSF1 by inhibiting the chaperone activity of Hsp70 (43), which may account for the lack of its therapeutic effect in our study. Importantly, 17-AAG has been shown to be less toxic than GA (29), which shows hepatotoxicity, and 17-AAG is currently being tested in clinical trials for the treatment of human cancer patients (44). In addition, intraperitoneal injection of 17-AAG into mice has been reported to induce multiple molecular chaperones in their spinal cord (45). Taken together, 17-AAG is the most promising therapeutic candidate for the polyQ diseases among the HSF1-activating compounds.

17-AAG has been reported to mitigate the neurological phenotypes of a mouse model of spinobulbar muscular atrophy by degradation of the mutant androgen receptor protein, an Hsp90 client protein, via its Hsp90 inhibitor activity, rather than by induction of molecular chaperones (45). In addition, Hsp90 inhibitors such as GA and RA have been reported to accelerate degradation of the mutant androgen receptor protein even in HSF1 knock-out cells (46), further supporting the possibility that the therapeutic effects of these Hsp90 inhibitors are not mediated by activation of HSF1 in the case of spinobulbar muscular atrophy models. Therefore, the effectiveness of Hsp90 inhibitors has been considered to be limited to spinobulbar muscular atrophy so far. In contrast, we show that knockdown of HSF1 abolished the induction of molecular chaperones and therapeutic effect of 17-AAG on polyQ-induced neurodegeneration in a *Drosophila* model of SCA3/MJD (Fig. 7), indicating that the therapeutic effect of 17-AAG depends on HSF1-mediated induction of molecular chaperones and not on degradation of the mutant MJD protein (Fig. 5*G*). Furthermore, we show that 17-AAG is also effective against neurodegeneration in a *Drosophila* model of Huntington disease (Fig. 3), consistent with a recent report showing that 17-AAG suppresses misfolding of the mutant huntingtin protein without its degradation (47). Therefore, we conclude that 17-AAG is effective against a wide range of polyQ diseases through HSF1-mediated induction of molecular chaperones.

In this study, we evaluated the therapeutic effects of HSF1-activating compounds on polyQ-induced neurodegeneration *in vivo*. We found that oral administration of 17-AAG markedly suppresses polyQ-induced neurodegeneration in *Drosophila* models of two polyQ diseases through HSF1-mediated induction of multiple molecular chaperones. Therefore, we conclude that 17-AAG is a promising therapeutic candidate for the polyQ diseases as well as other neurodegenerative diseases caused by protein misfolding.

*Acknowledgments—We thank M. Sone, H. Matsushima, R. Sasaki, and C. Ito for technical assistance. We thank Eisai Co. for providing GGA. We also thank N. M. Bonini for providing us with the MJDtr-Q27, MJDtr-Q78W, and MJDtr-Q78S fly lines; J. T. Littleton for the Htt-Q128 fly line; and the Bloomington Drosophila Stock Center and Drosophila Genetic Resource Center at Kyoto Institute of Technology for the other fly lines.*

## REFERENCES

1. Ross, C. A., and Poirier, M. A. (2005) *Nat. Rev. Mol. Cell Biol.* **6,** 891–898
2. Gusella, J. F., and MacDonald, M. E. (2000) *Nat. Rev. Neurosci.* **1,** 109–115
3. Zoghbi, H. Y., and Orr, H. T. (2000) *Annu. Rev. Neurosci.* **23,** 217–247
4. Bence, N. F., Sampat, R. M., and Kopito, R. R. (2001) *Science* **292,** 1552–1555
5. Nagai, Y., Onodera, O., Chun, J., Strittmatter, W. J., and Burke, J. R. (1999) *Exp. Neurol.* **155,** 195–203
6. Steffan, J. S., Kazantsev, A., Spasic-Boskovic, O., Greenwald, M., Zhu, Y. Z., Gohler, H., Wanker, E. E., Bates, G. P., Housman, D. E., and Thompson, L. M. (2000) *Proc. Natl. Acad. Sci. U. S. A.* **97,** 6763–6768
7. Steffan, J. S., Bodai, L., Pallos, J., Poelman, M., McCampbell, A., Apostol, B. L., Kazantsev, A., Schmidt, E., Zhu, Y. Z., Greenwald, M., Kurokawa, R., Housman, D. E., Jackson, G. R., Marsh, J. L., and Thompson, L. M. (2001) *Nature* **413,** 739–743
8. Kobayashi, Y., Kume, A., Li, M., Doyu, M., Hata, M., Ohtsuka, K., and Sobue, G. (2000) *J. Biol. Chem.* **275,** 8772–8778
9. Muchowski, P. J., Schaffar, G., Sittler, A., Wanker, E. E., Hayer-Hartl, M. K., and Hartl, F. U. (2000) *Proc. Natl. Acad. Sci. U. S. A.* **97,** 7841–7846
10. Chan, H. Y., Warrick, J. M., Gray-Board, G. L., Paulson, H. L., and Bonini, N. M. (2000) *Hum. Mol. Genet.* **9,** 2811–2820
11. Kazemi-Esfarjani, P., and Benzer, S. (2000) *Science* **287,** 1837–1840
12. Warrick, J. M., Chan, H. Y., Gray-Board, G. L., Chai, Y., Paulson, H. L., and Bonini, N. M. (1999) *Nat. Genet.* **23,** 425–428
13. Barth, P. (1996) *Proc. Natl. Acad. Sci. U. S. A.* **93,** 12418–12422
14. Muchowski, P. J., and Wacker, J. L. (2005) *Nat. Rev. Neurosci.* **6,** 11–22
15. Ishihara, K., Yamagishi, N., Saito, Y., Adachi, H., Kobayashi, Y., Sobue, G., Ohtsuka, K., and Hatayama, T. (2003) *J. Biol. Chem.* **278,** 25143–25150
16. Mitsui, K., Nakayama, H., Akagi, T., Nekooki, M., Ohtawa, K., Takio, K., Hashikawa, T., and Nukina, N. (2002) *J. Neurosci.* **22,** 9267–9277
17. Wyttenbach, A., Sauvageot, O., Carmichael, J., Diaz-Latoud, C., Arrigo, A. P., and Rubinsztein, D. C. (2002) *Hum. Mol. Genet.* **11,** 1137–1151
18. Zou, J., Guo, Y., Guettouche, T., Smith, D. F., and Voellmy, R. (1998) *Cell* **94,** 471–480
19. Baler, R., Dahl, G., and Voellmy, R. (1993) *Mol. Cell Biol.* **13,** 2486–2496
20. Chu, B., Soncin, F., Price, B. D., Stevenson, M. A., and Calderwood, S. K. (1996) *J. Biol. Chem.* **271,** 30847–30857
21. Fujikake, N., Nagai, Y., Popiel, H. A., Kano, H., Yamaguchi, M., and Toda, T. (2005) *FEBS Lett.* **579,** 3842–3848
22. Holmberg, C. I., Illman, S. A., Kallio, M., Mikhailov, A., and Sistonen, L. (2000) *Cell Stress Chaperones* **5,** 219–228
23. Xia, W., Vilaboa, N., Martin, J. L., Mestril, R., Guo, Y., and Voellmy, R. (1999) *Cell Stress Chaperones* **4,** 8–18
24. Fujimoto, M., Takaki, E., Hayashi, T., Kitaura, Y., Tanaka, Y., Inouye, S., and Nakai, A. (2005) *J. Biol. Chem.* **280,** 34908–34916
25. Westerheide, S. D., and Morimoto, R. I. (2005) *J. Biol. Chem.* **280,** 33097–33100
26. Yamanaka, K., Takahashi, N., Ooie, T., Kaneda, K., Yoshimatsu, H., and Saikawa, T. (2003) *J. Mol. Cell Cardiol.* **35,** 785–794
27. Warrick, J. M., Paulson, H. L., Gray-Board, G. L., Bui, Q. T., Fischbeck, K. H., Pittman, R. N., and Bonini, N. M. (1998) *Cell* **93,** 939–949
28. Lee, W. C., Yoshihara, M., and Littleton, J. T. (2004) *Proc. Natl. Acad. Sci. U. S. A.* **101,** 3224–3229
29. Page, J., Heath, J., Fulton, R., Yalkowsky, E., Tabibi, E., Tomaszewski, J., Smith, A., and Rodman, L. (1997) *Proc. Am. Assoc. Cancer Res.* **38,** 308

30. Schulte, T. W., Akinaga, S., Soga, S., Sullivan, W., Stensgard, B., Toft, D., and Neckers, L. M. (1998) *Cell Stress Chaperones* **3,** 100–108
31. Westerheide, S. D., Bosman, J. D., Mbadugha, B. N., Kawahara, T. L., Matsumoto, G., Kim, S., Gu, W., Devlin, J. P., Silverman, R. B., and Morimoto, R. I. (2004) *J. Biol. Chem.* **279,** 56053–56060
32. Warrick, J. M., Morabito, L. M., Bilen, J., Gordesky-Gold, B., Faust, L. Z., Paulson, H. L., and Bonini, N. M. (2005) *Mol. Cell* **18,** 37–48
33. Nollen, E. A., Garcia, S. M., van Haaften, G., Kim, S., Chavez, A., Morimoto, R. I., and Plasterk, R. H. (2004) *Proc. Natl. Acad. Sci. U. S. A.* **101,** 6403–6408
34. Auluck, P. K., Chan, H. Y., Trojanowski, J. Q., Lee, V. M., and Bonini, N. M. (2002) *Science* **295,** 865–868
35. Bruening, W., Roy, J., Giasson, B., Figlewicz, D. A., Mushynski, W. E., and Durham, H. D. (1999) *J. Neurochem.* **72,** 693–699
36. Cummings, C. J., Sun, Y., Opal, P., Antalffy, B., Mestril, R., Orr, H. T., Dillmann, W. H., and Zoghbi, H. Y. (2001) *Hum. Mol. Genet.* **10,** 1511–1518
37. Batulan, Z., Taylor, D. M., Aarons, R. J., Minotti, S., Doroudchi, M. M., Nalbantoglu, J., and Durham, H. D. (2006) *Neurobiol. Dis.* **24,** 213–225
38. Rujano, M. A., Kampinga, H. H., and Salomons, F. A. (2007) *Exp. Cell Res.* **313,** 3568–3578
39. Auluck, P. K., and Bonini, N. M. (2002) *Nat. Med.* **8,** 1185–1186
40. Kieran, D., Kalmar, B., Dick, J. R., Riddoch-Contreras, J., Burnstock, G., and Greensmith, L. (2004) *Nat. Med.* **10,** 402–405
41. Hay, D. G., Sathasivam, K., Tobaben, S., Stahl, B., Marber, M., Mestril, R., Mahal, A., Smith, D. L., Woodman, B., and Bates, G. P. (2004) *Hum. Mol. Genet.* **13,** 1389–1405
42. Katsuno, M., Sang, C., Adachi, H., Minamiyama, M., Waza, M., Tanaka, F., Doyu, M., and Sobue, G. (2005) *Proc. Natl. Acad. Sci. U. S. A.* **102,** 16801–16806
43. Otaka, M., Yamamoto, S., Ogasawara, K., Takaoka, Y., Noguchi, S., Miyazaki, T., Nakai, A., Odashima, M., Matsuhashi, T., Watanabe, S., and Itoh, H. (2006) *Biochem. Biophys. Res. Commun.* **353,** 399–404
44. Rutnen, E. A., Kondagunta, G. V., Ishill, N., Sweeney, S. M., Deluca, J. K., Schwartz, L., Bacik, J., and Motzer, R. J. (2006) *Invest. New Drugs* **24,** 543–546
45. Waza, M., Adachi, H., Katsuno, M., Minamiyama, M., Sang, C., Tanaka, F., Inukai, A., Doyu, M., and Sobue, G. (2005) *Nat. Med.* **11,** 1088–1095
46. Thomas, M., Harrell, J. M., Morishima, Y., Peng, H. M., Pratt, W. B., and Lieberman, A. P. (2006) *Hum. Mol. Genet.* **15,** 1876–1883
47. Herbst, M., and Wanker, E. E. (2007) *Neurodegener. Dis.* **4,** 254–260

J Hum Genet (2008) 53:1012–1015
DOI 10.1007/s10038-008-0336-5

SHORT COMMUNICATION

# *LRRK2* P755L variant in sporadic Parkinson's disease

**Hiroyuki Tomiyama · Ikuko Mizuta · Yuanzhe Li · Manabu Funayama · Hiroyo Yoshino · Lin Li · Miho Murata · Mitsutoshi Yamamoto · Shin-ichiro Kubo · Yoshikuni Mizuno · Tatsushi Toda · Nobutaka Hattori**

Received: 20 June 2008 / Accepted: 31 August 2008 / Published online: 16 October 2008


**Abstract** Parkinson's disease (PD) is a neurodegenerative disorder of unknown etiology with probable involvement of genetic-environmental factors. The majority of PD cases (approximately 90–95%) are sporadic, while familial cases account for approximately 5–10% of PD. In a recent report, a heterozygous *LRRK2* P755L mutation within *LRRK2* exon 19 was found in 2% of Chinese sporadic PD patients and in 0% of normal controls or Caucasians, suggesting that the mutation is disease-associated with ethnic specificity. To further evaluate the role of *LRRK2* P755L variant in sporadic PD, we performed direct sequencing of *LRRK2* exon 19 in 501 Japanese sporadic PD patients (male 249, female 252, aged 28–92 years, mean 65.0 years) and 583 controls of the Japanese general population as an extended association study. In this group, we found six patients (6/501 = 1.2%) and eight controls of the general population (8/583 = 1.6%) with a heterozygous P755L variant ($P = 0.80$, $\chi^2 = 0.064$). No other variants were found in exon 19. Together with previous reports, our extended case-controlled study of large sample size suggests that *LRRK2* P755L is a non-disease-associated polymorphism in PD patients.

**Keywords** Parkinson's disease · Genetics · *PARK8* · *Leucine-rich repeat kinase 2 (LRRK2)* · Polymorphism · Association study · Japanese · Ethnic background

H. Tomiyama · Y. Li · L. Li · S.-i. Kubo · N. Hattori (✉)
Department of Neurology,
Juntendo University School of Medicine,
2-1-1 Hongo, Bunkyo-ku, Tokyo 113-8421, Japan
e-mail: nhattori@med.juntendo.ac.jp

I. Mizuta · T. Toda
Division of Clinical Genetics,
Osaka University Graduate School of Medicine,
Suita, Japan

I. Mizuta · M. Murata · M. Yamamoto · T. Toda · N. Hattori
Core Research for Evolutional Science and Technology (CREST), Japan Science and Technology Agency,
Saitama, Japan

M. Funayama · H. Yoshino · Y. Mizuno
Research Institute for Diseases of Old Age,
Juntendo University School of Medicine, Tokyo, Japan

M. Murata
Department of Neurology, Musashi Hospital,
National Center of Neurology and Psychiatry, Tokyo, Japan

M. Yamamoto
Department of Neurology,
Kagawa Prefectural Central Hospital, Takamatsu, Japan

## Introduction

Parkinson's disease (PD, OMIM #168600) is the second most common neurodegenerative disorder next to Alzheimer's disease. The clinical features are characterized by levodopa-responsive parkinsonism, such as rigidity, resting tremor, bradykinesia, and postural instability. Although the cause of PD remains unclear, genetic-environmental interaction is suggested for the development of the disease. One of the autosomal-dominant forms of PD, *PARK8*, was originally mapped from a Japanese Sagamihara family (Funayama et al. 2002) and *LRRK2* (*PARK8*; *leucine-rich repeat kinase 2*, OMIM *609007) was identified as the causative gene for *PARK8*-linked PD (Paisán-Ruíz et al. 2004; Zimprich et al. 2004). Among *LRRK2* mutations, the most common *LRRK2* G2019S mutation in North Africans and Ashkenazi Jews has shown ethnic differences among Caucasian, Japanese, and Chinese (Nichols et al. 2005; Gilks et al. 2005; Lesage et al. 2006; Tomiyama et al.

2006; Tan et al. 2005). On the other hand, *LRRK2* G2385R variant has recently been found the most common genetic risk factor among Chinese and Japanese, but not Caucasians (Di Fonzo et al. 2006; Funayama et al. 2007; Tan et al. 2007; Farrer et al. 2007). Moreover, in a recent report (Wu et al. 2006), a heterozygous *LRRK2* p.P755L (c.2264c > *t*, rs34410987) mutation within *LRRK2* exon 19, corresponding to a predicted ankyrin-repeat-like domain of LRRK2, was found in 2% (12/598) of Chinese sporadic PD and 0% (0/765) of Chinese normal controls, suggesting its association with the disease. However, *LRRK2* P755L was reported as a polymorphism (3% of 92 normal controls) in the dbSNP database of Taiwanese. Thus, to determine the frequency and the role of *LRRK2* P755L in Asian PD, we screened for *LRRK2* exon 19 in Japanese sporadic PD patients.

## Subjects and methods

The nucleotide sequences of *LRRK2* exon 19 were determined by direct sequencing in 501 sporadic Japanese PD patients and 583 controls of the Japanese general population (Table 1). All blood samples and clinical information were obtained by the attending neurologists after obtaining informed consent from their patients. The study was approved by the ethics review committees of Juntendo and Osaka Universities. Diagnosis of PD was made by the attending neurologists based on the presence of parkinsonism and good response to anti-PD treatment. Controls of the Japanese general population were evaluated by neurologists to ensure none of them had PD. DNA was prepared using standard methods. They were amplified by polymerase chain reaction (PCR) of exon 19 and sequenced using BigDye Terminator Chemistry and ABI310 and 3130 Genetic Analyzer (Applied Biosystems, Foster City, CA). Sequences of the primers, conditions of PCR, and conditions of sequencing were based on a previous report (Zimprich et al. 2004).

## Results

We found 6 patients (6/501 = 1.2%) and 8 controls of the Japanese general population (8/583 = 1.6%) with a heterozygous P755L variant ($P = 0.80$, odds ratio = 1.15, 95% CI: 0.40–3.32, $\chi^2 = 0.064$) in *LRRK2* exon 19 (Table 2). No other variants were found in exon 19.

## Discussion

The purpose of the present study was to clarify the role of an ethnic-specific variant in the causative gene for PD. Although PD is considered a heterogeneous disease with genetic-environmental interaction, some cases certainly exhibit a Mendelian-inherited disease or are associated with strong genetic and ethnic background. Indeed, the reported frequency of *LRRK2* G2385R was higher in Asian sporadic PD patients than in controls (Di Fonzo et al. 2006; Funayama et al. 2007; Tan et al. 2007), although this is not the case in Caucasians. Moreover, Wu et al. (2006) in Nanjing, China, recently reported that a heterozygous *LRRK2* P755L mutation was found in 2% (12/598) of Chinese sporadic PD and 0% (0/765) of normal controls, whereas none (0/463) of the Caucasian PD patients had this mutation (Deng et al. 2007), suggesting ethnic differences, like *LRRK2* G2385R. However, our results of large case-controlled study in Japanese revealed that *LRRK2* P755L is a non-disease associated polymorphism. Consistent with our data, this variant was present at similar frequency in Taiwanese PD patients (7/578 = 0.99%) and Taiwanese normal controls (10/339 = 0.97%) (Di Fonzo et al. 2006). Furthermore, the latest report in the Chinese population in Singapore showed the absence of segregation and association of P755L with PD (case 4/204 = 2.0%, control 6/235 = 2.6%, $P = 0.76$) (Tan et al. 2008). These findings might be based on ethnic or native differences in human migration history or human genetics.

We reported previously that the most common *LRRK2* G2019S mutation in Mendelian-inherited and sporadic PD

**Table 1** Profile of analyzed samples in this study

| Parameter | Patients | Controls of general population |
|---|---|---|
| Total sample, *n* (%) | 501 (100) | 583 (100) |
| Male, *n* (%) | 249 (49.7) | 312 (53.5) |
| Female, *n* (%) | 252 (50.3) | 271 (46.5) |
| Age at sampling (years)[a] | 65.0 ± 9.6 (28–92) | 45.0 ± 17.0 (21–98) |
| Male[a] | 64.3 ± 10.2 (28–92) | 43.6 ± 15.0 (22–92) |
| Female[a] | 65.4 ± 9.9 (28–92) | 46.8 ± 19.0 (21–98) |
| Age at onset (years)[a] | 58.0 ± 10.5 (20–88) | |
| Male[a] | 57.7 ± 10.9 (20–88) | |
| Female[a] | 58.3 ± 10.1 (25–82) | |

[a] Data are mean ± SD (range)

**Table 2** Allele frequency of *LRRK2* c. 2264C > T (p. P755L) in Japanese patients with Parkinson's disease and controls of general population

| | Genotype, *n* (%) | | | Allele, *n* (%) | | | |
|---|---|---|---|---|---|---|---|
| | C/C | C/T | T/T | C | T | $\chi^{2a}$ | OR (95% CI) |
| Patients ($n = 501$) | 495 (98.8) | 6 (1.2) | 0 (0) | 996 (99.4) | 6 (0.6) | 0.06 | 1.15 (0.40–3.32) |
| Controls of general population ($n = 583$) | 575 (98.6) | 8 (1.4) | 0 (0) | 1,158 (99.3) | 8 (0.7) | | |

[a] Compared with the control

*OR* odds ratio, *CI* confidence interval

was rare in Asians compared to North Africans or Caucasians (Tomiyama et al. 2006). *LRRK2* variants are reported to spread worldwide with some ethnic differences among each variant, such as R1441G, R1441C, R1441H (exon 31, ROC domain), G2019S, I2020T (exon 41, MAPKKK domain), and G2385R (exon 48, WD40 domain) (Mata et al. 2005). Since *LRRK2* consists of as many as 51 exons, it is important to decide which exon(s) of this gene should be screened first for efficient analysis of mutation in patients with various ethnic backgrounds. In this regard, *LRRK2* exon 41 and 31 are reasonable to be screened first; however, exon 19 is not likely a candidate exon for causative mutation screening in PD. In addition, although MAPKKK and ROC domain are reported to be associated with kinase activity of LRRK2 (Paisán-Ruíz et al. 2004; Zimprich et al. 2004; Smith et al. 2006), the existence and the role of the predicted ankyrin repeat-like domain in LRRK2 have not been established yet.

So far, *LRRK2* P755L as well as G2385R variants have been found in only Chinese, Taiwanese, and Japanese (Asians) with similar frequencies in some Asians, but have not been found in Caucasians. Thus, these variants could occur independently in very ancient Asians with a single founder effect (Farrer et al. 2007). Although the HapMap project has been very successful, the presence of ethnic differences among *LRRK2* variants such as G2019S, R1441G, G2385R, and P755L suggest that further establishment of ethnic-specific or native-specific data is essential for more accurate SNP analyses and genome-wide association studies.

## Conclusion

Our extended association study in Japanese with large sample size suggests that *LRRK2* P755L is a non-disease-associated polymorphism in PD patients.

**Acknowledgments** The authors thank all the participants. The authors also thank Ms. Yuko Nakabayashi and Ms. Yoko Imamichi for the excellent technical assistance. This work was supported by a grant from Core Research for Evolutional Science and Technology (CREST) of the Japan Science and Technology Agency (JST) and by Grants-in-Aid from the Research Committee of CNS Degenerative Diseases, the Ministry of Health, Labor, and Welfare of Japan.

## References

Deng H, Le W, Huang M, Xie W, Pan T, Jankovic J (2007) Genetic analysis of LRRK2 P755L variant in Caucasian patients with Parkinson's disease. Neurosci Lett 419:104–107

Di Fonzo A, Wu-Chou YH, Lu CS, van Doeselaar M, Simons EJ, Rohé CF, Chang HC, Chen RS, Weng YH, Vanacore N, Breedveld GJ, Oostra BA, Bonifati V (2006) A common missense variant in the LRRK2 gene, Gly2385Arg, associated with Parkinson's disease risk in Taiwan. Neurogenetics 7:133–138

Farrer MJ, Stone JT, Lin CH, Dächsel JC, Hulihan MM, Haugarvoll K, Ross OA, Wu RM (2007) Lrrk2 G2385R is an ancestral risk factor for Parkinson's disease in Asia. Parkinsonism Relat Disord 13:89–92

Funayama M, Hasegawa K, Kowa H, Saito M, Tsuji S, Obata F (2002) A new locus for Parkinson's disease (PARK8) maps to chromosome 12p11.2–q13.1. Ann Neurol 51:296–301

Funayama M, Li Y, Tomiyama H, Yoshino H, Imamichi Y, Yamamoto M, Murata M, Toda T, Mizuno Y, Hattori N (2007) Leucine-rich repeat kinase 2 G2385R variant is a risk factor for Parkinson disease in Asian population. NeuroReport 18:273–275

Gilks WP, Abou-Sleiman PM, Gandhi S, Jain S, Singleton A, Lees AJ, Shaw K, Bhatia KP, Bonifati V, Quinn NP, Lynch J, Healy DG, Holton JL, Revesz T, Wood NW (2005) A common LRRK2 mutation in idiopathic Parkinson's disease. Lancet 365:415–416

Lesage S, Durr A, Tazir M, Lohmann E, Leutenegger AL, Janin S, Pollak P, Brice A, French Parkinson's Disease Genetics Study Group (2006) LRRK2 G2019S as a cause of Parkinson's disease in North African Arabs. N Engl J Med 354:422–423

Mata IF, Kachergus JM, Taylor JP, Lincoln S, Aasly J, Lynch T, Hulihan MM, Cobb SA, Wu RM, Lu CS, Lahoz C, Wszolek ZK, Farrer MJ (2005) Lrrk2 pathogenic substitutions in Parkinson's disease. Neurogenetics 17:1–7

Nichols WC, Pankratz N, Hernandez D, Paisán-Ruíz C, Jain S, Halter CA, Michaels VE, Reed T, Rudolph A, Shults CW, Singleton A, Foroud T, Parkinson Study Group-PROGENI investigators (2005) Genetic screening for a single common LRRK2 mutation in familial Parkinson's disease. Lancet 365:410–412

Paisán-Ruíz C, Jain S, Evans EW, Gilks WP, Simón J, van der Brug M, López de Munain A, Aparicio S, Gil AM, Khan N, Johnson J, Martinez JR, Nicholl D, Carrera IM, Pena AS, de Silva R, Lees A, Martí-Massó JF, Pérez-Tur J, Wood NW, Singleton AB (2004) Cloning of the gene containing mutations that cause PARK8-linked Parkinson's disease. Neuron 44:595–600

Smith WW, Pei Z, Jiang H, Dawson VL, Dawson TM, Ross CA (2006) Kinase activity of mutant LRRK2 mediates neuronal toxicity. Nat Neurosci 9(10):1231–1233

Tan EK, Shen H, Tan LC, Farrer M, Yew K, Chua E, Jamora RD, Puvan K, Puong KY, Zhao Y, Pavanni R, Wong MC, Yih Y, Skipper L, Liu JJ (2005) The G2019S LRRK2 mutation is uncommon in an Asian cohort of Parkinson's disease patients. Neurosci Lett 384:327–329

Tan EK, Zhao Y, Skipper L, Tan MG, Di Fonzo A, Sun L, Fook-Chong S, Tang S, Chua E, Yuen Y, Tan L, Pavanni R, Wong MC, Kolatkar P, Lu CS, Bonifati V, Liu JJ (2007) The LRRK2 Gly2385Arg variant is associated with Parkinson's disease: genetic and functional evidence. Hum Genet 120:857–863

Tan EK, Lim HQ, Yuen Y, Zhao Y (2008) Pathogenicity of LRRK2 P755L variant in Parkinson's disease. Mov Disord (online 8 Feb 2008)

Tomiyama H, Li Y, Funayama M, Hasegawa K, Yoshino H, Kubo S, Sato K, Hattori T, Lu CS, Inzelberg R, Djaldetti R, Melamed E, Amouri R, Gouider-Khouja N, Hentati F, Hatano Y, Wang M, Imamichi Y, Mizoguchi K, Miyajima H, Obata F, Toda T, Farrer MJ, Mizuno Y, Hattori N (2006) Clinicogenetic study of mutations in *LRRK2* exon 41 in Parkinson's disease patients from 18 countries. Mov Disord 21:1102–1108

Wu T, Zeng Y, Ding X, Li X, Li W, Dong H, Chen S, Zhang X, Ma G, Yao J, Deng X (2006) A novel P755L mutation in LRRK2 gene associated with Parkinson's disease. NeuroReport 17:1859–1862

Zimprich A, Biskup S, Leitner P, Lichtner P, Farrer M, Lincoln S, Kachergus J, Hulihan M, Uitti RJ, Calne DB, Stoessl AJ, Pfeiffer RF, Patenge N, Carbajal IC, Vieregge P, Asmus F, Müller-Myhsok B, Dickson DW, Meitinger T, Strom TM, Wszolek ZK, Gasser T (2004) Mutations in LRRK2 cause autosomal-dominant parkinsonism with pleomorphic pathology. Neuron 44:601–607

ORIGINAL CONTRIBUTION

# Mutation Analysis of the *PINK1* Gene in 391 Patients With Parkinson Disease

*Ryuya Kumazawa, MD; Hiroyuki Tomiyama, MD; Yuanzhe Li, MD; Yoko Imamichi; Manabu Funayama, PhD; Hiroyo Yoshino, BS; Fusako Yokochi, MD, PhD; Toshihiro Fukusako, MD, PhD; Yasushi Takehisa, MD; Kenichi Kashihara, MD; Tomoyoshi Kondo, MD, PhD; Bulent Elibol, MD, PhD; Sevasti Bostantjopoulou, MD; Tatsushi Toda, MD, PhD; Hirohide Takahashi, MD; Fumihito Yoshii, MD, PhD; Yoshikuni Mizuno, MD; Nobutaka Hattori, MD, PhD*

**Objectives:** To determine the frequency, distribution, and clinical features of Parkinson disease (PD) with *PINK1* mutations.

**Design:** Retrospective clinical and genetic review.

**Setting:** University hospital.

**Patients:** We performed extensive mutation analyses of *PINK1* in 414 PD patients negative for *parkin* mutations (mean [SD] age at onset, 42.8 [14.3] years), including 391 unrelated patients (190 patients with sporadic PD and 201 probands of patients with familial PD) from 13 countries.

**Results:** We found 10 patients with PD from 9 families with *PINK1* mutations and identified 7 novel mutations (2 homozygous mutations [p.D297MfsX22 and p.W437R] and 5 single heterozygous mutations [p.A78V, p.P196QfsX25, p.M342V, p.W437R, and p.N542S]). No compound heterozygous mutations were found. The frequency of homozygous mutations was 4.26% (2 of 47) in families with autosomal recessive PD and 0.53% (1 of 190) in patients with sporadic PD. The frequency of heterozygous mutations was 1.89% (2 of 106) in families with potential autosomal dominant PD and 1.05% (2 of 190) in patients with sporadic PD. The mean (SD) age at onset in patients with single heterozygous mutations (53.6 [11.1] years; range, 39-69 years) was higher than that in patients with homozygous mutations (34.0 [20.3] years; range, 10-55 years). Myocardial iodine-123 metaiodobenzylguanidine uptake was low in patients with heterozygous mutations but not in those with homozygous mutations.

**Conclusions:** Our results suggest that homozygous *PINK1* mutations tend to be diagnosed as the early-onset autosomal recessive form of PD. Single heterozygous mutations may contribute to the development of sporadic PD and also could be an additional genetic predisposition for developing familial PD. The reduced myocardial iodine-123 metaiodobenzylguanidine uptake observed in patients with single heterozygous *PINK1* mutations is similar to that seen in patients with sporadic PD.

*Arch Neurol. 2008;65(6):802-808*

PARKINSON DISEASE (PD) IS PREDOMINANTLY characterized by degeneration of midbrain dopaminergic neurons, eventually leading to various motor dysfunctions, such as rigidity, tremor, bradykinesia, and postural instability.[1] The etiology of PD is unknown but is presumably multifactorial, eg, perhaps having a genetic × environmental interaction.

Although most PD cases are sporadic, several causative genes have been identified in recent years in familial forms of PD. For example, *alpha-synuclein* (loci, *PARK1* and *PARK4*), *UCH-L1* (*PARK5*), and *LRRK2/dardarin* (*PARK8*) are reported to be the causative genes for autosomal dominant PD (ADPD)[2-6]; and *parkin* (*PARK2*), *DJ-1* (*PARK7*), and *PINK1* (OMIM 608309) (*PARK6*) are reported to be the causative genes for autosomal recessive PD (ARPD).[7-9] Mutations in *parkin* are the major cause of ARPD, and the frequency of such mutations in families with ARPD is approximately 50%.[10] In contrast, mutations in *DJ-1* are rare (≤ 1%) in ARPD.[11] Increasing numbers of patients with *PINK1* mutations are being reported; however, there are no sufficiently large studies to define the frequency, age distribution, or clinical features of patients with PD associated with *PINK1* mutations worldwide, especially not in Asia. Moreover, no association between PD and coding single nucleotide polymorphisms within *PINK1* has been reported.[12] The role of a single heterozygous *PINK1* mutation in the clinical manifestation of parkinsonism, such as age at onset, is not clear at present, mainly because previous reports have not identified substantial num-

Author Affiliations are listed at the end of this article.

**Table 1. Characteristics of 414 Analyzed Patients With Parkinson Disease**

| Type of Disease | No. of Patients | Mean (SD) Age at Onset, Range, y |
|---|---|---|
| Sporadic Parkinson disease | 190 (105 males, 85 females) | 37.2 (10.4), 7-81 |
| Familial Parkinson disease | 224 (201 probands, 23 relatives; 100 males, 124 females) | 47.6 (15.5), 10-85 |
| ARPD | 55 (47 probands) | 52.8 (13.8) |
| ADPD | 121 (106 probands) | 47.1 (15.8) |
| Unclear hereditary information | 48 | 43.1 (16.0) |
| Total | 414 (391 unrelated patients [190 patients with sporadic disease and 201 probands]) | 42.8 (14.3) |

Abbreviations: ADPD, autosomal dominant Parkinson disease; ARPD, autosomal recessive Parkinson disease.

bers of *PINK1* mutations. To clarify these aspects, we performed extensive mutation analysis in a large number of patients with PD in 13 countries.

## METHODS

### PATIENTS

We studied 414 *parkin*-negative PD patients (391 unrelated patients and 23 relatives) from 13 countries (249 Japanese, 55 Korean, 28 Israeli, 27 Taiwanese, 27 Chinese, 14 Tunisian, 5 Turkish, 3 Greek, 2 Moroccan, 1 Filipino, 1 Bulgarian, 1 Brazilian, and 1 Australian individual). Patients received clinical diagnoses of PD[13] regardless of their familial history. The distribution of age at onset was as follows: younger than 50 years (early-onset) (n=287 [69.3%]), 50 years or older (late-onset) (n=117 [28.3%]), and unknown (n=10 [2.4%]). Hereditary information and the mean ages at onset of patients with PD are provided in **Table 1**. In this study, we defined mode of inheritance as autosomal recessive (≥2 affected siblings in only 1 generation) and autosomal dominant (≥1 affected member in 2 consecutive generations). All participants in the control cohort were Japanese individuals. The study was approved by the ethics review committee of Juntendo University. Blood samples for genetic analysis and clinical information were collected by local neurologists after obtaining informed consent from the patients.

### GENETIC ANALYSIS

Genomic DNA was isolated from peripheral blood using standard protocols. For direct sequence analysis, DNA was amplified by polymerase chain reaction of each exon, using standard methods and published primers.[14] Dideoxy sequencing was performed with Big Dye Terminator Chemistry (Applied Biosystems, Foster City, California). These products were loaded on ABI 377, ABI 310, and ABI 3130 automated DNA sequence analyzers (Applied Biosystems) and analyzed with DNA Sequence Analysis software (Applied Biosystems). *Parkin* mutations were examined by polymerase chain reaction, direct sequencing, and quantitative assays based on real-time polymerase chain reaction with TaqMan probes (Applied Biosystems) in each exon. We ruled out *parkin* mutations including exonic deletions or multiplications by dosage studies before analysis of *PINK1*. For extensive screening of substitutions and to determine whether or not the novel *PINK1* mutations were pathogenic, we performed direct sequencing in 300 chromosomes of healthy control DNA samples for all coding exons. All controls were evaluated by neurologists to ensure none of them had parkinsonism.

### GENE DOSAGE STUDIES

We performed polymerase chain reaction–based exon dosage assay using TaqMan Chemistry and an ABI PRISM 7700 sequence detection system (Applied Biosystems) in the 5 patients who had a heterozygous *PINK1* mutation (patients E, F, G, H, and J) to rule out compound heterozygous mutations with other heterozygous exonic deletion or multiplication. We used the primer and the probe of Assay by Design (Applied Biosystems) according to a previously published report.[14]

### MYOCARDIAL IODINE-123 METAIODOBENZYLGUANIDINE SCINTIGRAPHY

Myocardial iodine-123 metaiodobenzylguanidine ($^{123}$I-MIBG) scintigraphy was performed in 5 *PINK1* mutation–positive patients (from different hospitals) with an intravenous injection of 111 MBq of $^{123}$I-MIBG (Daiichi Radioisotope Laboratories, Tokyo, Japan). Early images were obtained 15 minutes and delayed images were obtained 3 to 4 hours after injection. Whole myocardial $^{123}$I-MIBG uptake was measured on a planar image as the early and delayed heart to mediastinum activity ratio.

### STATISTICAL ANALYSIS

Data are expressed as mean (SD). For continuous variables, such as age at onset, the *t* test was used to test for significant differences between the 2 groups. Categorical data, such as individual responses to each question on the diagnosis checklist and frequencies, were compared with the $\chi^2$ test, with Yates correction when appropriate.

## RESULTS

### GENETIC ANALYSIS

We identified 10 patients with PD from 9 families with *PINK1* mutations, including 7 novel mutations (**Table 2**). Three homozygous missense mutations were found in 4 patients: p.T313M, p.C388R, and a novel p.W437R. Previously, p.T313M and p.C388R had been reported.[15,16] In addition, 3 novel single heterozygous missense mutations were found in 4 patients: p.A78V, p.M342V, and p.N542S. We also identified 1 novel homozygous deletion (p.D297MfsX22) and 1 novel single heterozygous deletion (p.P196QfsX25). We also found 1 patient with familial PD (without clear mode of inheritance) with a novel single heterozygous variant (p.V482M).

**Table 2. Clinical Features of Study Patients With *PINK1* Mutations**

| Measure | Missense Mutations | | | | | | | | Homozygous Deletion | Heterozygous Deletion |
|---|---|---|---|---|---|---|---|---|---|---|
| | Homozygous | | | | Heterozygous | | | | | |
| Patient | A | B | C | D | E | F | G | H | I | J |
| Nucleotide change | c.938C→T | c.1162T→C | c.1162T→C | c.1309T→C | c.233C→T | c.1024A→G | c.1024A→G | c.1625A→G | c.889delG | c.585delC |
| Amino acid change | p.T313M | p.C388R | p.C388R | p.W437R | p.A78V | p.M342V | p.M342V | p.N542S | p.D297MfsX22 | p.P196QfsX25 |
| Exon | 4 | 6 | 6 | 7 | 1 | 5 | 5 | 8 | 4 | 2 |
| Heredity form | SPD | ARPD | ARPD | FPD | SPD | SPD | ADPD | ADPD | ARPD | FPD |
| Country of residence | Japan | Japan | Japan | Turkey | Japan | Japan | Japan | Japan | Greece | Japan |
| Consanguinity | – | – | – | – | – | – | – | – | + | – |
| Age at onset, y | 32 | 55 | 54 | 19 | 39 | 49 | 53 | 69 | 10 | 58 |
| Disease duration, y | 2 | 10 | 2 | 21 | 21 | 12 | 4 | 7 | 15 | 16 |
| Sex | M | F | F | F | F | F | M | F | F | F |
| Resting tremor | – | – | – | – | – | – | + | + | + | + |
| Rigidity | – | – | – | – | – | + | – | + | + | – |
| Bradykinesia | – | – | – | – | – | + | + | + | – | – |
| Postural instability | – | – | – | – | – | – | – | – | + | – |
| Gait disturbance | – | – | – | – | – | – | – | + | + | + |
| Frozen gait | – | – | – | – | – | – | – | – | – | – |
| Wearing off | – | – | – | – | – | + | – | + | + | – |
| On/off states | – | – | – | – | – | + | – | – | + | NA |
| Asymmetry at onset | – | – | + | – | – | + | – | + | – | – |
| Orthostatic hypotension | – | – | – | – | – | – | – | – | – | – |
| Incontinence | – | – | – | – | – | – | – | – | – | – |
| Urinary urgency | – | – | – | – | – | – | – | – | – | – |
| Levodopa-induced dyskinesia | – | – | – | – | – | – | – | – | – | – |
| Sleep benefit | – | – | + | – | – | – | – | – | – | – |
| Dystonia at onset | – | – | – | – | – | – | – | – | – | – |
| Hyperreflexia | – | – | – | – | – | – | – | – | – | + |
| Dementia | – | – | – | – | – | – | – | + | – | – |
| Depression | – | – | – | – | – | – | – | – | – | – |
| Hallucinations | – | – | – | – | – | + | – | – | – | – |
| Other psychosis | – | – | – | – | – | – | – | – | – | – |
| UPDRS score, on/off states | 19/39 | 18/NA | NA/6 | 16/22 | NA | NA | NA | NA | 77/NA | 64/259 |
| Hoehn-Yahr stage | | | | | | | | | | |
| On state | 2 | 2 | 1 | 1.5 | 2.5 | 4 | 3 | 2 | 2 | 3 |
| Off state | 3 | NA | NA | 2.5 | NA | NA | NA | 3 | 4 | NA |
| Myocardial $^{123}$I-MIBG uptake | NA | Not decreased | Not decreased | NA | Decreased | NA | NA | Decreased | NA | Decreased |
| Early H:M activity ratio (standard value) | NA | 1.82 (> 1.45) | 1.97 (> 1.45) | NA | 1.49 (> 1.45) | NA | NA | 1.4 (> 1.84) | NA | 1.64 (> 2.2) |
| Delayed H:M activity ratio (standard value) | NA | 2.93 (> 1.45) | 1.97 (> 1.45) | NA | 1.25 (> 1.45) | NA | NA | 1.18 (> 1.78) | NA | 1.28 (> 2.2) |

Abbreviations: ADPD, autosomal dominant Parkinson disease; ARPD, autosomal recessive Parkinson disease; FPD, familial Parkinson disease (definite information on mode of inheritance not available, though some family members had parkinsonism); H:M, heart to mediastinum; NA, not applicable or no information available; SPD, sporadic Parkinson disease; UPDRS, Unified Parkinson Disease Rating Scale; +, present; –, absent; $^{123}$I-MIBG, iodine-123 metaiodobenzylguanidine.

We did not find any of these mutations or variants in 300 chromosomes in a healthy Japanese population, and we did not detect exonic deletion or multiplication by gene dosage study. The aforementioned novel missense mutations and variant have not been reported as polymorphisms. In addition, we examined the homology regarding the *PINK1* protein. The site of p.W437R mutation was highly conserved among various species. On the other hand, the p.V482M variant was not highly conserved (data not shown).

The affected relatives of patients G, H, and J could not be tested for cosegregation of the same heterozygous mutation that was found in the probands. Thus, we could not exclude that the mutation does not cosegregate in 1 or more of these families. No cosegregation of the p.V482M variant was observed among patients in the same family. Therefore, the role of this variant in this family was not clear.

The frequency of homozygous *PINK1*-positive patients was 1.02% (4 of 391 [1 patient with sporadic PD + 3 familial PD probands]/[190 patients with sporadic PD + 201 familial PD probands]) among the entire group of PD patients. Furthermore, the frequency of homozygous *PINK1*-positive patients was 4.26% (2 of 47) in ARPD families and 0.53% (1 of 190) in patients with sporadic PD. Homozygous mutations were not detected in patients with ADPD. However, the frequency of single heterozygous *PINK1*-positive patients was 1.28% (5 of 391) among the entire group of PD patients, 1.89% (2 of 106) in ADPD families, and 1.05% (2 of 190) among patients with sporadic PD. No single heterozygous mutations were detected in patients with ARPD.

## CLINICAL ANALYSIS

Table 2 lists the clinical features of 10 *PINK1*-positive patients and the **Figure** shows the pedigree of families with the *PINK1* mutation. In this study, the family with no cosegregation of p.V482M was excluded from Table 2 and the Figure, because the role of the V482M variant in this

family was not clear. Among the *PINK1*-positive families, consanguineous marriages were noted in 5 patients (patients B, C, D [pedigree not available], I, and J).

The mean age at onset of patients with homozygous *PINK1* mutations was 34.0 (20.3) years (range, 10-55 years), and that of patients with a single heterozygous *PINK1* mutation was 53.6 (11.1) years (range, 39-69 years). The age at onset was significantly lower in the homozygous *PINK1*-positive patients compared with the single heterozygous *PINK1*-positive and *PINK1*-negative patients.

As presented in Table 2, motor dysfunction was comparatively mild in many *PINK1*-positive patients. The mean Hoehn-Yahr stage of homozygous *PINK1*-positive patients was 1.7 (0.4) in the on state and 3.3 (0.6) in the off state. In contrast, the average Hoehn-Yahr stage of patients with a single heterozygous *PINK1* mutation was 2.9 (0.5) in the on state and 3.0 (0.0) in the off state. Even in patient E, who had had PD for 21 years, the Hoehn-Yahr stage was 2.5. None of the patients had a Hoehn-Yahr stage of 5.0.

Patient I had a homozygous 1-base deletion mutation and patient J had a single heterozygous 1-base deletion mutation. These 2 patients had similar deletion mutations that caused stop codons within the serine/threonine kinase domain of *PINK1*, but age at onset was clearly different: 58 years for patient J (the latest) and 10 years for patient I (the earliest among *PINK1*-positive patients). Although both patients had hyperreflexia, patient J did not have dystonia at onset, while patient I had dystonia at onset. To date, none of the *PINK1*-positive patients in this study were investigated pathologically.

### MYOCARDIAL $^{123}$I-MIBG SCINTIGRAPHY

Myocardial $^{123}$I-MIBG scintigraphy was performed in 5 *PINK1*-positive patients (patients B, C, E, H, and J). The early and delayed heart to mediastinum ratios of these patients are listed together with the age-matched standard values in Table 2. Myocardial $^{123}$I-MIBG uptake was normal in patients with homozygous *PINK1* mutations (patients B and C), whereas it was decreased in patients with single heterozygous *PINK1* mutations (patients E, H, and J).

## COMMENT

Combining the results of our previous studies[14,15,17] and this study, the frequency of *PINK1*-positive families with 2 allele mutations (homozygous mutations and compound heterozygous mutations) among *parkin*-negative ARPD was 11.5% (10 of 87). Among heterozygous mutations, many were single heterozygous rather than compound heterozygous. Our results showed that not only a Japanese individual but 1 Greek and 1 Turkish individual had *PINK1* mutations (Table 2), which suggests that the mutation is possibly distributed worldwide, similar to *parkin* mutations.[10,11] Considering previous reports on the frequencies of *parkin*[10,11] and *DJ-1*[18,19] mutations, we propose that we should first screen patients with PD for *parkin* mutations, including gene dosage

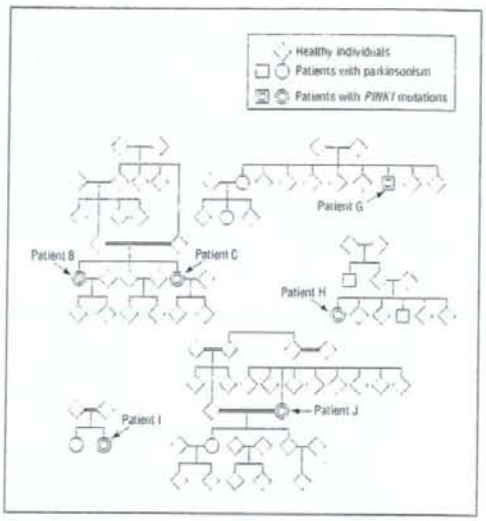


**Figure.** Pedigrees of patients with *PINK1* mutations. Patients B and C had the same homozygous missense mutation (p.C388R) in exon 6. Patient G had a single heterozygous mutation (p.M342V) in exon 5. Patient H had a single heterozygous mutation (p.N542S) in exon 8. Patient I had a homozygous deletion mutation (p.D297MfsX22) in exon 4, and patient J had a single heterozygous deletion mutation (p.P196QfsX25) in exon 2. The sexes are concealed to safeguard the confidentiality of the family members.

study, then screen for *PINK1* mutations, and finally screen for *DJ-1* in ARPD.

In the present study, we did not screen fully for heterozygous *PINK1* deletion mutations and multiplications by the gene dosage study using TaqMan assay to save time in screening all patients. Homozygous *PINK1* deletion mutation of more than 1 exon structure had been reported in only 1 case so far.[15] *PINK1* and *DJ-1* deletion mutations seem to be less frequent than *parkin* deletion mutations even if these heterozygous deletion mutations are to be included. In this regard, we think that gene dosage study of *PINK1* may not be as important as that of *parkin*.

Although the prevalence was rare, our study and others[20-22] showed that homozygous mutations as well as single heterozygous *PINK1* mutations are found not only in ARPD but also in ADPD families and patients with sporadic PD. These results suggest that screening for *PINK1* mutations may also be necessary in patients with potential ADPD and sporadic PD.

Although heterozygous carriers are clinically unaffected in most autosomal recessive disorders, higher preponderance of heterozygous *PINK1* mutations in patients with sporadic PD, compared with matched controls, has been reported.[21-23] Accordingly, although it is difficult to make a firm conclusion about the frequencies of heterozygous *PINK1* mutations in patients vs controls, all the single heterozygous *PINK1* mutations were found only in Japanese patients with PD but not in Japanese controls. Moreover, in the positron-emission tomographic study, carriers of heterozygous *PINK1* mutations showed significant reductions in caudal and putaminal fludeoxyglucose F18 uptake (mean of 20%-30% lower than the controls), indicating increased susceptibility for the de-

**Table 3. Clinical Features of 23 Patients With *PINK1* Mutations in Current and Past Studies**

| Measure | No. of Patients | | | | | *P* Value | | |
|---|---|---|---|---|---|---|---|---|
| | | *PINK1*-Mutation Positive | | | | | | |
| | No *PINK1* Mutation (n=404) | Homozygous (n=16) | Compound Heterozygous (n=2) | Heterozygous (n=5) | All (n=23) | 2 Mutations vs 1 Mutation | 2 Mutations vs No Mutation | Mutation Positive vs No Mutation |
| Sporadic PD | 187 | 1 | 0 | 2 | 3 | | | |
| ARPD[a] | 52 | 14 | 2 | 0 | 16 | | | |
| ADPD | 119 | 0 | 0 | 3 | 3 | | | |
| Patients with familial PD, unclear hereditary information | 46 | 1 | 0 | 0 | 1 | | | |
| Age at onset, mean (SD), y | 42.8 (14.3) | 32.6 (8.5) | 18.5 (0.7) | 53.6 (11.1) | 35.9 (15.0) | .001 | .001 | .03 |
| Resting tremor | 293 | 11 | 2 | 5 | 18 | .47 | .83 | .72 |
| Rigidity | 366 | 13 | 2 | 5 | 20 | .82 | .54 | .83 |
| Bradykinesia | 368 | 12 | 2 | 5 | 19 | .62 | .14 | .32 |
| Postural instability | 244 | 9 | 0 | 4 | 13 | .49 | .53 | .88 |
| Gait disturbance | 268 | 15 | 1 | 5 | 21 | .91 | .08 | .02 |
| Frozen gait | NA | 9 | 0 | 1 | 10 | .49 | NA | NA |
| Wearing off | 227 | 11 | 2 | 2 | 15 | .42 | .27 | .53 |
| On/off states | NA | 9 | 0 | 1 | 10 | .49 | NA | NA |
| Asymmetry at onset | 293 | 9 | 1 | 3 | 13[b] | .64 | .34 | .26 |
| Orthostatic hypotension | 43 | 2 | 0 | 2 | 4[c] | .57 | .99 | .30 |
| Incontinence | 30 | 1 | 0 | 2 | 3[b] | .23 | .81 | .52 |
| Urinary urgency | 63 | 2 | 0 | 2 | 4[b] | .44 | .93 | .98 |
| Levodopa-induced dyskinesia | 170 | 6 | 2 | 1 | 9 | .51 | .96 | .95 |
| Sleep benefit | 112 | 6 | 2 | 0 | 8 | .14 | .20 | .62 |
| Dystonia at onset | 53 | 3 | 1 | 0 | 4 | .62 | .45 | .79 |
| Hyperreflexia | 51 | 8 | 0 | 1 | 9 | .50 | .001 | .001 |
| Dementia | 41 | 2 | 0 | 0 | 2 | .91 | .79 | .90 |
| Depression | NA | 2 | 0 | 0 | 2 | .91 | NA | NA |
| Hallucinations | 62 | 2 | 0 | 2 | 4 | .40 | .88 | .97 |
| Other psychosis | 26 | 1 | 0 | 0 | 1 | .48 | .73 | .97 |
| Hoehn-Yahr stage, mean (SD) | | | | | | | | |
| On state | 2.5 (1.0) | 2.3 (0.7) | NA | 2.9 (0.5) | 2.5 (0.7) | .06 | .29 | .48 |
| Off state | 3.4 (1.1) | 2.9 (0.9) | NA | 3.0 (0.0) | 3.3 (1.1) | NA | .27 | .24 |

Abbreviations: ADPD, autosomal dominant Parkinson disease; ARPD, autosomal recessive Parkinson disease; NA, not applicable; PD, Parkinson disease.
[a] Thirteen of the patients with ARPD were reported previously by our group.[12,16,17]
[b] n=22.
[c] n=19.

velopment of parkinsonism.[24] In addition, our data showed that the age at onset of patients with heterozygous *PINK1* mutations was higher than that of patients with homozygous *PINK1* mutations and was similar to that of classic sporadic PD. Thus, the previous findings and our data emphasize the importance of heterozygous *PINK1* mutations as a possible risk factor for developing the common classic form of sporadic PD. However, we could not exclude other possibilities, eg, that these mutations could be coincidental findings or even be a cause of ADPD, because we did not perform the genetic tests in the relatives of the patient with a single heterozygous mutation or in controls outside of the Japanese population. In addition, we could not exclude the possibility of digenic inheritance or technical limitations in detecting all possible mutations (eg, in the introns and promoter).

**Table 3** lists the clinical symptoms of the patients in this study and patients reported previously by our group.[14,15,17] Thus, we could compare 23 *PINK1*-positive patients with 404 *PINK1*-negative patients and compare 18 patients with 2 allele *PINK1* mutations (16 patients with homozygous *PINK1* mutations and 2 patients with compound heterozygous mutations) with 5 patients with 1 allele *PINK1* mutation. The data in Table 3 show that most *PINK1*-positive patients develop early-onset parkinsonism. Moreover, the mean age at onset of patients with 1 allele *PINK1* mutation was higher than that of patients with 2 allele mutations.

Age at onset, hyperreflexia, and gait disturbances were significantly more frequent in homozygous *PINK1*-positive patients than in *PINK1*-negative patients. Indeed, these symptoms were also significantly different in patients with or without *PINK1* mutations. However, there were no statistical differences in pathognomonic symptoms between patients with 1 or 2 allele *PINK1* mutations, except for age at onset. These data indicate that the phenotypes of patients with a single heterozygous *PINK1* mutation are more likely to be similar to those of homozygous *PINK1*-positive patients, except for age at onset.

Myocardial $^{123}$I-MIBG scintigraphy is one of the most supportive diagnostic tools used in differentiating PD from